Structural, physical and optical properties of rice husk ash derived glass/ceramics

A thesis submitted for the partial fulfillment of the requirement for

the award of the degree of

Master of Technology

in

Materials & Metallurgical Engineering

Submitted by:

GAURAV SHARMA

Roll No. 601102013

Under the guidance of

Dr. KULVIR SINGH

(Professor and Head)

SCHOOL OF PHYSICS & MATERIALS SCIENCE

THAPAR UNIVERSITY, PATIALA

(PUNJAB) 147004

JULY 2013

DEDICATED TO MY LOVING PARENTS AND MY TEACHERS

Certificate

This is to certify that the thesis entitled "**Structural, physical and optical properties of rice husk ash derived glass/ceramics**" submitted by **Mr. Gaurav Sharma** in the partial fulfillment of the requirement for the award of the degree of Masters of Technology in **Materials & Metallurgical Engineering** from the School of Physics and Materials Science, Thapar University, Patiala, is a record of candidate's own work carried out by him under my supervision and guidance. The matter of this report has not been submitted in part or full to any University or institution for the award of any degree.

Supervisor:

Dr. Kulvir Singh

(Professor and Head)

School of Physics and Materials Science

Thapar University, Patiala

Countersigned by:

Dr. Kulvir Singh

(Professor and Head),

School of Physics and Materials Science

Thapar University, Patiala

Dr. S.K. Mohapatra

(Dean, Acedmic Affair),

Mechanical Engineering Department,

Thapar University, Patiala

ACKNOWLEDGEMENT

At this momentous occasion of binding my thesis I would like to acknowledge the contribution of all those benevolent people, I have been blessed to associate with. All the data collection, theories model would have failed to serve purpose for me if blessing of God would not have joined hands with my efforts.

My first and foremost offering of thanks goes to the architect who shaped my dreams into reality, my guide and mentor **Dr. Kulvir Singh** (Professor and Head), School of Physics and Materials Science, Thapar University, Patiala for perseverance, exuberance, positive approaches are just some of the traits he imprinted on my personality. He steered me through his journey through his invaluable advice, positive criticism, stimulating discussion and consistent encouragement. His meticulous attention towards my proceedings, his devoted time and his ideas has enabled me to make the project a success. His faith in me has always made me more confident. His blessing always made me optimistic. If I will stand proud of my achievements then undeniably he is the main creditor. It had been my privilege to work under his tutelage.

I would like to express my sincere thanks to **Dr. O. P. Pandey** (Senior Professor), School of Physics and Materials Science, Thapar University, Patiala. He has been very helpful in improving my dissertation. I am grateful to him for sharing his time and expertise. His comments and views were very insightful and helpful.

My special thanks to all the faculty of School of Physics and Materials Science who were always helpful to me throughout my work.

My special thanks to P. G. Lab Superintendent **Mr. Purushottam Singh** and **Mr. Jant Singh**, for providing all kind of assistance in PG Lab for creating a healthy research environment.

I would like to give my special thanks to Research Scholars **Paramjyot Jha, Satwinder Singh, Samita Thakur, Gourav Singla, Mani Mahajan** and **Pooja Singla** for guiding me at various stages of my experimental work.

I would also like to give many thanks to other Research Scholars **Kapil Sood, Ranvir Singh, Chandni Khurana, Jagdeep Kaur, Parveen Kumar Jha, Pallavi Gupta, Sakshi Gupta,**

Sunil Kumar Arya, Suresh Kumar, Manpreet Kaur and **Mintu Tyagi** for any kind of help and valuable suggestion whenever I needed out of their busy schedule.

I would also like to thank to Research Scholars **Mohit Sharma** and **Veeresh Vishnoi** for helping me in conducting some of the experiments at Department of Materials science, NIT Hamirpur (HP).

I would also like to thank my all friends and my colleagues specially **Amit Choudhary, Shashank Sharma, Shalini Rajput** and **Rupanjit Grewal** at the Materials & Metallurgical Engineering program and the School of Physics and Materials Science are acknowledged for providing me a friendly atmosphere and encouraging me throughout this research.

Last but not the least, My heartiest thanks to my parents for their moral support that kept my spirit up during the endeavor.

Gaurav Sharma

Roll No. 601102013

Abstract

The environmental problem is the greatest concern for scientific community all over the world. Utilization of the waste materials thus, is drawing major interest of the scientific research community. Many developed and developing nations are using industrial and agricultural waste for various applications. The agricultural wastes are being used in various applications to prevent the environmental problem for instance fly ash is being used in the civil construction, like to make the house and roads due to their low density, low weight without compromising their mechanical properties. Similarly rice husk and rice husk ash (RHA) is being used in various applications like in ceramic and refractory industry, glass industry, artificial jewelry, steel industry, cement and construction industry etc. RHA is being used as filler for high strength & low density composites. It is helpful in potential applications in gamma-ray shielding. It can be used as an effective adsorbent for various applications. In most of the countries sugarcane leaves, in general are used to make the comfort fertilizers, to make the rough paper in some extent. Particularly, farmers burn the leaves and it will create the environmental problem. The waste that otherwise would be harmful for the environment, can be safely and successfully used for potential applications. Also it reduces production cost. Some reports have been appearing in the literature to make the glass and glass ceramics using rice husk ash after giving some chemical treatment. Nobody has reported to make the glasses using rice husk ash and sugar cane leave ash. Attempts have been made to synthesize glass and glass ceramics from the rice husk ash to make the glasses taking different content of both the constituents. It is really worthwhile to investigate the effect of sugar cane leave ash on the formation of the glasses, their structure, thermal and optical properties. The as prepared glass and products are characterized using X-ray diffraction, Dilatometery, Raman spectroscopy, FT-IR and UV-spectroscopy.

List of Abbreviations

XRD	X-ray Diffractometry
SEM	Scanning Electron Microscopy
FTIR	Fourier Transform Infra-Red
RHA	Rice husk ash
SCLA	Sugarcane leaves ash
RHA-Fe	Iron incorporated rice husk ash
LOI	Loss of Ignition
HDPE	High density polyethylene
RRH	Raw rice husk
HSO	Hydroxy silicone oil
HMS	Hexa-methyldisilazane
MTS	Methyl triethoxysilane
CTE	Coefficient of linear thermal expansion
DIL	Dilatometer
Ru-RHA	Ruthenium rice husk ash
IC	Initial concentration
PVA	Poly vinyl alcohol
UV/Vis.	Ultra violet/visible spectroscopy
CBR	California bearing ratio
ASR	alkali-silica reaction
MMC	Metal matrix composite

Contents

INDEX

List of tables

List of figures

Chapter-1

Introduction

Rice husk and sugar cane leaves are agricultural waste materials that are produced in huge amount every year. This causes various environmental problems. Utilization of the waste materials is attracting much interest of the scientific community all around the world. In this chapter, the physical, structural, chemical and optical properties of rice husk ash and sugar cane leaf ash have been discussed.

1.1 Rice

Rice is the seed of the monocot plants *Oryza sativa* (Asian rice) or *Oryza glabaerreima* (African rice). Rice is grown in all worlds except Antarctica. Rice cultivation is the principle activity to provide food of the million persons of the world and also the source of the income for many families. Several countries of Asia and Africa are highly dependent on the rice as a food. Rice is the second most consumed food after maize in all over the world. Asia is the dominating continent for production of rice. About 90 % of rice supply of the world is generated by Asia [1].

In all the plant residues, the ash of rice husk contains the highest proportion of silica. On the other hand, rice husk ash obtained from the incineration of husk, which is rich in silica (87-97 %) with small amounts of alkali and other trace elements. Silica in Rice Husk Ash (RHA) exists in amorphous or crystalline form, depending upon the production conditions. Each form of silica has a different structure depending upon the reactivity. RHA has several applications in silicon based industries, apart from extensive uses in the field of Civil Engineering [2].

1.2 Production of rice husk

Rice husk is a potential material, which is amenable for value addition. It is extensively used either in its raw form or in ash form. Most of the husk from the milling is either burnt or dumped as waste in open fields and a small amount is used as fuel for boilers, electricity generation, bulking agents for composting of animal manure etc. The presence of amorphous silica is concentrated at the surfaces of the rice husk and not within the husk itself [3].

The chemical composition of rice husk is similar to that of many common organic fibers**.** The chemical composition of rice husk is reported by some groups [4]. One of the compositions is mentioned below:

Table 1.1 The chemical composition of rice husk as organic fibers.

Rice husk	**Range (%)**
Cellulose	40-50
Lignin	25-35
Ash	15-20
Moisture	8-15

After burning, most evaporable components are slowly lost and the silicates are left. Inorganic materials are found in the form of free salts and particles of cationic groups combined with the anionic groups of fiber into the plants [5].

Table 1.2 The typical properties of rice husk.

Property	**Range (%)**
Hardness (Mohr's scale)	5-6
Bulk density (kg/m^3)	96-160
Hydrogen	4-5
Carbon	≈ 35
Oxygen	31-37
Nitrogen	0.23-0.32
Ash	22-29
Sulphur	0.04-0.08
Moisture	8-9

The content of each of these depends on rice variety, soil chemistry, climatic conditions and even the geographical localization of the agriculture.

1.3 Thermal decomposition of rice husk

There are two distinct stages in the decomposition of rice husk carbonization and de-carbonation. Carbonization is the decomposition of volatile matter in rice husk at temperatures greater than 300°C and releases combustible gas and tar. De-carbonation is the combustion of fixed carbon in the rice husk char at higher temperatures in the presence of oxygen [6].

1.4 Applications of rice husk

Suitability of Rice husk (RH) to be used for different applications depends upon the physical and chemical properties of the husk such as ash content, silica content etc. The direct use of rice husk as fuel has been seen in power plants. Apart from this, RH uses as a source of raw material for the synthesis and development of new phases and compounds. A detailed description related to application of rice husk in industrial sectors as well as other fields is given below:

1.4.1 As fuel in power plant

Rice husk is mostly used as fuel in boilers for processing paddy and generation of process steam. Heat energy is produced through direct combustion or by gasification. Small sector process industries use fixed low capacity boilers, which are manually fired using rice husk as a fuel. It has been seen that to produce 1MWh, approximately 1 ton of rice husk is required. So, the technical and economic factors decide the effective use of rice husk as fuel for power generation. Moreover, rice husk has been used as a fuel for household energy [7].

1.4.2 Formation of activated carbon

Due to the presence of large amounts of hydrocarbon such as cellulose and lignin content, rice husk can be used as a raw material to prepare activated carbons which are complex porous structures. They are obtained by two different processes: the physical or thermal activation and the chemical activation. In the former, carbonization is followed by char activation; while in the later one, carbonization and activation are performed in a single step, using a chemical agent.

Physical activation of rice husk produces activated carbon that exhibits very low specific area. Activated carbons are effective adsorbents due to their micro-porous structure [8].

1.4.3 Use as source of silica and silicon compounds

Apart from organic component, the presence of up to 20 % silica makes rice husk a promising raw material source for a number of silicon compounds such as silicon carbide, silicon nitride, silicon tetrachloride, zeolite, silica and pure silicon. The applications of such materials derived from rice husk are very comprehensive [9].

1.4.4 Porous SiO_2/C composite from rice husk

During heat treatment of RH in inert atmosphere, organic compounds decompose and partly change to H_2O, CO, CO_2 and volatile compounds, remaining carbon and SiO_2 [10].

1.4.5 Insulating fire brick using rice husk

Bricks made by using rice husk develop plenty of pores during heat treatment due to burning out of organic material [11]. The more the percentage of rice husk in a brick, the more porous would be the brick and better thermal insulation. The presences of entrapped air in pores have thermal insulating characteristics and thus make the porous fire brick structure suitable for backup insulation.

1.5 Rice husk ash production technology

1.5.1 Properties of rice husk

Rice husk is unusually high in ash compared to other biomass fuels in the range 10-20 %. The RHA is 87-97 % silica highly porous and lightweight and with a very high external surface area [12]. Presence of high amount of silica makes it a valuable material for use in industrial applications. Other constituents of RH after the burning conditions, such as K_2O, Al_2O_3, CaO, MgO, Na_2O and Fe_2O_3 are available in less than 1 %. The silica in the ash undergoes structural transformations depending on the conditions of combustion such as time and temperature [13]. It is already reported that burning rice husk at controlled conditions below 700 °C yielded amorphous ash and temperatures greater than 800 °C resulted in crystalline ash. The temperatures exceeding 700 °C could also yield reactive amorphous ash, but the duration of

incineration should be short [6, 14]. Other investigators also concluded that the combustion environment affects a specific surface area of RHA [15]. Therefore time, temperature and environment must be carefully selected in the pyro processing of rice husks to ensure ash of maximum reactivity [16].

1.5.2 Thermal treatment technologies

The thermal treatment technology, which has been widely used to produce amorphous silica from rice husk are fluidized bed combustor, rotary kiln and industrial furnace.

1.5.2.1 Fluidized bed combustor:

Production of pozzolanic RHA can also be done by combustion of rice husk using fluidised bed combustors. It encompasses a range of combustion/boiler combinations where combustion of the fuel takes place within a bed of inert material that is kept "fluid" by an upward draught of air. The combustion chamber is similar to conventional boilers, such as stoker fired designs, except that the floor of the boiler is covered with numerous air nozzles and some ash removal outlets. In the process, the heat from the combustion of rice husk has utilized to produce steam or electricity. The limitations of fluidized bed combustors are as follows:

1. The relatively high pressure drop is required to fluidise a bed:
2. The flue gas carries a high dust load etc.

1.5.1.2 Rotary kiln:

The use of rotary kiln for producing amorphous silica from rice husk is an innovation in the muffle furnace concept in order to provide some degree of mixing to the rice husk. The system, which comprises of two rotary kilns in tandem, was patented by Sugita and offers a method for producing amorphous rice husk ash [18].

1.5.2.3 Furnace:

In the early periods, muffle furnace has been used for the RHA production. Silica from rice husk ash was prepared by heating rice husk in a laboratory muffle furnace at temperatures ranging from 500-1150 ^{OC} [16].

1.6 Effect of various parameters on properties of RHA

There is a wide range in the physical and chemical properties of RHA. The chemical and physical properties of the ash may be influenced by the soil chemistry, paddy variety and fertilizer use. The change from amorphous to crystalline ash occurs at approximately 800 ºC, although the process is often 'incomplete' until 900 ºC is achieved. All the combustion processes devised to burn rice husks remain below 1440 ºC, which is the RHA melting temperature. Global production of RHA is about 25 million tons a majority of it is coming from countries in Southeast Asia [17]. A few studies have shown that the physical and chemical properties of ash are dependent on the soil chemistry, paddy variety and climatic conditions. The differences may also arise due to fertilizers applied during rice cultivation [6, 17].

1.7 Determination of amorphous silica in rice husk ash

Rice husk ash have large amount of silica after the burning, which can be very use full for as a silica source. And after this type of utilization of rice husk ash (RHA) can solve the problem of waste materials. There are two ways for determination silica in rice husk ash given below.

1.7.1 Analytical method

Some specific analytical methods are available to evaluate the amorphous silica content in RHA. The degree of the amorphousness of silica is estimated by calculating the percentage of available silica that is dissolved in an excess of boiling 0.5 M sodium hydroxide in a three minute extraction period [17]. The reactivity of RHA towards lime, different masses up to 0.3 g of RHA in increments of 0.025 g was placed in 100 ml beakers [18]. To each, 50 ml of 21.5 molar calcium hydroxide solutions was added and the contents of the beakers were kept out of contact with atmospheric carbon-di-oxide. After 100 hours, the solutions were analyzed for un-reacted calcium ions a rapid analytical method based on bringing the siliceous non-crystalline fraction of pozzolan into solution as glycero-silicate [19]. Standard test methods for evaluating reactive silica are somewhat tedious and time consuming, since these include stages of filtration, calcinations etc.

1.7.2 Instrumental techniques

Apart from the analytical methods, there are some instrumental techniques employed to identify the amorphous/crystalline state of silica in RHA. X-ray diffraction technique can be used to study the crystalline fraction of the material. Nuclear magnetic resonance (NMR) technique probes the local structure of a silicon atom and is therefore a powerful technique to characterize amorphous silica [20].

1.8 Physical characteristics of RHA

Over the years, researchers have tried to characterize pozzolanas i.e. Fly ash based on its physical properties such as specific gravity, fineness and grain size distribution and have attempted to relate these properties to its activity. But for RHA, no such specific research is conducted to relate the physical parameters to its activity.

1.8.1 Particle size distribution

RHA is a porous material consisting of irregular or angular shaped particles. Some particles may also be spherical in nature [4]. The median particle size of about 8 μm is required to achieve pozzolanic activity index of 100 % [21]. In general, particles below 45 μm in size can actively take part in the pozzolanic reaction [22].

1.8.2 Fineness

Generally, reactivity of a medium is favored by increasing the fineness of the reacting materials. But, reactivity of RHA is attributed to its high content of amorphous silica and its porous nature [23]. RHA is porous in nature has an extremely high surface area while its average size still remains fairly high. Compared to silica fume with average particle size of 0.1 μm, RHA with particle size around 45 μm will have three times higher surface area [24]. Prolonged burning will cause collapse of the cellular form and also coalescence of the fine pores, which consequently causes a reduction in surface area. At higher temperatures with prolonged burning, a crystalline structure is formed with a sharp reduction in surface area expressed that fineness of RHA increases with increase in grinding time for all burning temperatures [25].

1.8.3 Specific gravity and density

Specific gravity of RHA varies in a narrow range of 2.02-2.16 and its bulk density varies in the range of 112 to 202 kg /m^3 [26].

1.8.4 Color

Color changes are associated with the completeness of the combustion process as well as structural transformation of silica in the ash. Ash in white color is an indication of a complete oxidation of the carbon, which is also an indication of availability of a large portion of amorphous silica in the ash. At high temperatures, strong interaction between potassium and silica ions cause the formation of potassium poly silicate combined with carbon resulting in gray color ash [1]. If the husk is pretreated with acid, a major portion of its potassium will be removed due to which ash will not attain gray color [17]. Temperatures still at higher levels along with prolonged burning will result in ash with lilac pink color, representative of silica in crystalline form such as cristobalite and tridymite. The above three colors distinctly stand for amorphous, transition and crystalline states of ash formation [27].

1.9 Chemical composition of RHA

Table 1.3 The Chemical composition of RHA [12, 13].

Chemical composition	**RHA (%)**
SiO_2	91
Al_2O_3	0.35
Fe_2O_3	0.41
MgO	0.81
SO_3	1.21
P_2O_5	0.98
Na_2O	0.08
K_2O	3.21
Loss of Igination	8.5

1.9.1 Loss of ignition

Typically, RHA contains some un-burnt components as well as inert components of the husk. The un-burnt component is predominantly carbon. Loss on ignition, the weight loss of ash burned at temperatures less than 1000 °C is related to the presence of carbonates, combined water in residual clay minerals and combustion of free carbon.

1.9.2 Oxide composition

All the constituents of RHA, except potassium and magnesium, are present in a very small range, that is, less than 1 %. In India, the samples from two southern places Trivandrum and Hyderabad, appears to be high in magnesium, aluminum and iron oxide content. The use of chemical fertilizers in the paddy field may be contributing to this, in addition to the difference in the soil chemistry [23].

1.10 Microstructural and crystal studies of RHA

The introduction of sophisticated instruments in the field of material characterization has enabled detailed structural studies of any material. It revealed that, up to 500 °C, ash particles are spherical or globular in shape and with porous structure. Partially crystallized ash was found at 600 °C [28]. X-ray Diffraction studies revealed that RHA predominantly with amorphous silica exhibited broad peak centered on 2θ angle of 22° [29, 30]. When Silicon di-oxide is at pure state, cristobalite and tridymite forms of silica are detected at temperatures greater than about 1427 ^{o}C. At atmospheric pressure, tridymite and cristobalite are crystallised at 867-1470 ^{o}C and 1470-1727 ^{o}C, respectively [31]. However, due to the presence of impurities in rice husk, the transition from amorphous to crystalline forms (cristobalite and tridymite) occurs at a much lower temperature.

1.11 Application of RHA

Rice husk ash has been widely used in various industrial applications such as processing of steel, cement, refractory industry etc. Suitability of RHA mainly depends on the chemical composition of ash, predominantly silica content in it. RHA is found to be superior to other supplementary materials like slag, silica fume and fly ash.

1.11.1 RHA is used in steel industries

RHA is used during the production of high quality flat steel [32]. The ash also finds application as an excellent insulator, having fine insulating properties including low thermal conductivity, a high melting point, low bulk density and high porosity. RHA is also used as a coating over the molten metal in the 'tundish' and in ladle which acts as a very good insulator and does not allow quick cooling of metal.

I. RHA is used by the steel industry in the production of high quality flat steel. Flat steel is a plate product or a hot rolled strip product, typically used for automotive body panels and domestic 'white goods' products.
II. RHA is an excellent insulator, having low thermal conductivity, high melting point, low bulk density and high porosity. It is this insulating property that makes it as an excellent ' tundish powder'. These powders that are used to insulate the tundish prevent rapid cooling of the steel and ensure uniform solidification in the continuous casting process.

1.11.2 RHA as silica

Due to the presence of large silica content in ash, extraction of silica is economical. Silica is also precipitated in customized forms to meet the requirements of various uses. Some of the uses of silica are in rubber industry as reinforcing agent, in cosmetics, in toothpastes as a cleansing agent and in the food industry as an anti-caking agent [33]. There is a growing demand for fine amorphous silica in the production of high performance cement and concrete, use in bridges, marine environments, nuclear power plants etc.

1.11.3 Use in ceramics and refractory industries

Rice husk ash is used in the manufacture of refractory bricks because of its insulating properties. It has been used in the manufacture of low-cost, lightweight insulating boards. RHA has been used as a silica source for cordierite production. Replacement of kaolinite with rice husk silica in the mixture composition, yields higher cordierites with a lower crystallize temperature and decrease in activation energy of crystallization [34].

1.11.4 Rubber manufacturing

Due to the similarity in surface area and surface activity, the RHA (both low-carbon and high-carbon contents) can be classified as inert filler which could be used in the rubber industry for economical purposes. When incorporated into rubber, the ash, regardless of its carbon content, imparts the compound with low viscosity and faster vulcanization because of the presence of metal oxides. The modulus and hardness of the ash-filled vulcanizetes are comparable to those of the vulcanizetes filled with other commercial inert fillers [35].

1.11.5 Paint industry

Rice husk ash is used as improves the stability of paint. RHA gives the more durability and strength using into the paint.

1.11.6 Use as cosmetics

The rice husk ash glass and glass ceramics have been used as making the artificial beauty product. There are many types of vassals and beauty product made by RHA.

1.11.7 RHA in cement and construction industries

Substantial research has been carried out on the use of amorphous silica in the manufacture of concrete. There are two areas for which RHA is used, in the manufacture of low cost building blocks and in the production of high quality cement. RHA is used as a mineral additive to improve performance of concrete. Reports indicated RHA as a highly reactive pozzolan [36].

1.11.8 Silicon chips making by RHA

Biocon in Australia has carried out work on purifying amorphous RHA but can only get to about 99.9 % purity at a great cost and Biocon consider that there are no real market opportunities with silicon chips [37]. However The Indian Space Research Organization has successfully developed technology for producing high purity precipitated silica from RHA and this has a potential use in the computer industry. The consortium of American and Brazilian scientists has also developed ways to extract and purify silicon with the aim of using it in semiconductor manufacture [38]. A

company in Michigan is purifying RHA into silica suitable for several industries, including silicon chip manufacture [39].

1.12 Sugarcane

Sugar cane is a perennial plant of the *genus Saccharum*. Sugar cane is the world's largest crop and is grown in more than 100 countries [40]. Brazil, India, China, Thailand, Mexico and Australia are major contributors to the world's sugarcane production [41]. The composition of sugar cane depends very much on the cane variety, the region and the climatic conditions under which it is grown, the degree of maturity of the cane. The sugar cane plant can be divided into three parts: root stalk and leaves [42]. Typically, sugarcane is grown for sugar production. Sugarcane is also a feedstock for ethanol production. Residues from sugarcane plantations include bagasse, leaves and tops. The bagasses are traditionally used as a fuel in the sugar factories to generate electricity for their own usage.

Sugar cane is composed mainly of sucrose, fiber and water, usually in the proportions of about 12, 15 and 70 % by weight, respectively.

1.13 Applications of sugar cane leaves

The leaves and tops are mostly burnt in the fields and are not efficiently used for energy. Only a small part of the leaves and tops are used as a compost and animal feed. Approximately 500 million tons per year leaves and tops are produced [43]. These biomass residues could be used for energy production by thermo chemical conversion processes such as combustion, gasification and pyrolysis.

1.14 Chemical composition of sugar cane leaves ashes

Chemical composition of the sugar cane leaves ash has been determined and reported by some research groups [44]. The following table represents the composition of sugar cane leave ash.

Table1.4 Chemical compositions of sugar cane leave ash [45].

SCLA	Chemical composition (%)
SiO_2	74.74
Al_2O_3	1.87
Fe_2O_3	0.48
CaO	6.39
MgO	2.42
K_2O	2.37
Na_2O	0.15
TiO_2	0.10
SO_3	1.30

1.15 Applications of sugarcane leaf ash

(a) Use as a fertilizer in field

(b) Use as a source of silica

(c) Use as cement and constructions

1.16 Effect of burning of sugarcane leaves on Environment

Although it is primarily grown for the production of sugar, current focus on sustainable energy and sound environmental practices have led to the realization that lingo cellulosic biomass such as that derived from sugar cane can form the basis of a bio-refinery with a wide range of possible products [45]. The recent drop in the worldwide price of sugar in 2012 has also spurred an increased interest in other uses of the sugar cane plant. Because the sugar cane plant is a perennial C_4 grass it is a highly efficient converter of solar radiation into biomass, more so than wheat or maize.

Chapter-2

Literature review

The main problem with agricultural waste materials is with their disposal or storage. Burning these wastes cause many harmful environmental problems. Many research groups have been working on the utilization of the waste materials for potential applications. Literature on the production and applications of the RHA and RHA derived materials are reviewed. Some of the reports on the concerned topic are given below:

Mehta [46] concluded that maintaining the combustion temperature below 500 °C under oxidizing conditions for prolonged periods or temperature up to 680 °C with less than one minute could produce amorphous silica. Prolonged heating above this temperature may cause the material to convert, at least in part to, crystalline silica; first to cristobalite and then tridymite.

Hamad *et al.* [47] identified the temperature range of 500 to 700 °C as optimum for reactive ash formation. Electrical conductivity tests verify the good pozzolanic activity of the RHA 500 and RHA 700 samples, with uniformly higher values for the samples incinerated at 500 °C. XRD and microscopic analysis confirmed the amorphous character of both the RHA 500 and RHA 700 samples with the first crystalline material appearing at processing temperatures of 900 °C and higher.

Chopra *et al.* [48] reported that for incineration temperatures up to 700 °C the silica was predominantly in amorphous form and the crystals present in the ashes grew with the increase in time of burning.

James *et al*. [49] performed a systematic study of RHA processing and its reactivity. They indicated that isothermal heating at a minimum of 402 °C is required for complete destruction of organic matter from rice husk and to liberate silica. On combustion, the cellulose-lignin matrix burns away, leaving a porous silica skeleton; this can be ground to a fine powder with high surface area.

Surana *et al*. [50] have introduced a simple conductometric technique for measuring the activity of pozzolanic materials based on the dissolution of 200 mg of pozzolana sample in 0.7 percent

hydrofluoric acid solution and measuring the conductivity after 30 minutes. The specific conductivity is directly correlated to the amount of silica present in the samples.

Hiemstra *et al*. [51] have been investigated that the dissolution of silica is strongly influenced by their surface structure where the charge of the surface plays an important role depending on the binding or the release of protons at Si-OH surface groups.

Wang *et al*. [52] observed that zeolite ZSM-48 with a very high sensitivity 99.9 % can be synthesized from a reaction mixture containing a silica source from rice husk ash.

Yu *et al.* [53] concluded that C-S-H gel is formed by a dissolution-precipitation process where the silica in RHA is quickly dissolved in the high pH $Ca(OH)_2$ solution and subsequently $gCa1.5SiO_{3.5}\ xH_2O$ precipitates.

Saha *et al.* [54] studied the possibility by using RHA for manufacturing activated carbon, and confirmed its usefulness in water purification. Attempts have been made to utilize RHA in vulcanizing rubber. RHA has been shown to offer advantages over silica as a vulcanizing agent for ethylene-propylene-di-inter-polymer (EPDM), and is recommended as diluents filler for EPDM rubber.

Huang *et al.* [55] developed a thermal model to obtain reactive RHA from rice husk in a fluidized bed. Another study on the combustion of rice husk in a circulating fluidized bed reported that a fluidizing velocity of 1.2 m/s and air split in 7:3 are reasonable to obtain combustion efficiency of above 97 %.

Asavapisit *et al*. [56] conducted tests by burning husk at different temperatures ranging from 400-800 °C for one-hour duration and reported that the temperature of 650 °C could be used for producing Ru-RHA based on a strength activity index.

The porous SiO_2/C composites with a high surface area by heating the pellets in inert atmosphere fabricated **Watari *et al*** [57]. Porous SiO_2/C composite was able to be fabricated through a simple one-step firing process. The pore characteristics of the products could be controlled by changing the molding pressure raw, RH particle size, and heat treatment temperature. Heating at 1000 ºC displayed the optimal properties such as 87 % porosity, 450 m^2/g specific surface areas, Larger RH particles resulted in products with higher strength.

Nair *et al.* [58] determined the applicability of rice husk ash (RHA) as a pozzolanic material. Silica in RHA formed by burning rice husk in a laboratory furnace under continuous supply of air has been characterized as a function of particular temperature, time and cooling rate. This sample showed the highest conductivity drop in the pozzolanic activity test. It concluded that the most reactive rice husk ashes are produced after incineration for 12 h at 500 °C.

The morphological analysis of RHA ceramics shows that the microstructure of samples was related to the phase of crystal occurred. On the other hand, EDX analysis confirms the composition of elements contain in RHA ceramics. But most research has been focused on the formation of cristobalite and tridymite **Kordatos *et al***. [59].

Nayak *et al*. [60] developed a procedure for obtaining and characterizing active blue silica from rice husk ash. About 25 wt. % silica powder (from the total mass of rice husk) of 95 % pure silica could be produced after heat-treating at 700 °C for 6 h. The sharp color changing from blue to pink of the dried blue silica gel of amorphous characteristics was obtained at 3 % moisture absorption, and total moisture adsorption capacity was 39.5 % at 80 % RH. The results show that this novel preparation procedure provides an easy pathway to produce blue silica gel from rice husk according to specification.

Bhavornthanayod *et al.* [61] observed that the burning of rice husk in air results in the formation of rice husk ash (RHA) with a content in SiO_2 that varies from 85 to 98 % depending on the burning conditions, the furnace type and the rice variety. The thickness of zeolite was directly affected by the synthesis time.

Rukzon *et al*. [62] analyzed that the effect of grinding on the chemical and physical properties of rice husk ash was studied. As the fineness's of the rice husk ash increases, the specific gravity also increases indicates that grinding is most effective for the increase in the fineness of the original rice husk ash. The increase in grinding time and the fineness of rice husk ash decreases the water demand of the mix.

Lakshmi *et al*. [63] explored the adsorptive characteristics of Indigo Carmine (IC) dye from aqueous solution onto rice husk ash (RHA). Batch experiments were carried out to determine the influence of parameters like initial pH (pH_0), contact time (t), adsorbent dose (m) and initial concentration (C_0) on the removal of IC. The interaction processes were accompanied by an

increase of entropy value. They concluded that the RHA could be employed as low-cost adsorbent for the removal of dye from aqueous solution.

Jennifer *et al.* [64] worked on actual conditions during sugarcane burning on commercial estates, investigate the physical-chemical properties of the cultivated leaves and ash products, and quantify the presence of crystalline silica. Commercially grown raw sugarcane leaf was found to contain up to 1.8 weight % silica, mostly in the form of amorphous silica bodies (with trace impurities e.g., Al, Na, Mg), with only a small amount of quartz. The sugarcane trash ash formed after pre-harvest burning contained between 10 and 25 wt % SiO_2, mostly in an amorphous form, but with up to 3.5 wt % quartz. Both quartz and cristobalite were identified in the sugarcane bagasse ash (5-15 wt % and 1-3 wt %, respectively) formed in the processing factory. Electron microprobe analysis showed trace impurities of Mg, Al and Fe in the silica particles in the ash. The absence of crystalline silica in the airborne emissions and lack of cristobalite in trash ash suggest that high temperatures during pre-harvest burning were not sustained long enough for cristobalite to form, which is supported by the presence of low temperature sylvite and calcite in the residual ash.

Adam *et al.* [65] silica-tin material has been synthesized by simple sol-gel method using rice husk ash as the source of silica and cetyl-tri-methyl-ammonium bromide as the surfactant at room temperature. The materials were calcination at 500 ^{o}C for 5 h gave nanotubes with external diameter of 2-4 nm and internal diameter of 1-2 nm. The BET specific surface area was found to be 607m^2/g. The powder X-ray diffraction pattern showed that the material is amorphous. The photo-catalytic activity of the prepared material was studied towards degradation of methylene blue under UV-irradiation. According to the experimental results the silica–tin nanotubes exhibit high photo-catalytic activity compared to pure rice husk silica.

Haslinawati *et al.* [66] studied that two forms of crystal phase, cristobalite and tri-dymite contained in RHA ceramic presented. Raw material (RHA) heat treated in order to produce white ash powder. The results showed that the RHA ceramic sintered at 1000 °C contained a high percentage of cristobalite and this continues decreasing as the temperature increasing. It seems to be different from tridymite phase where it becomes greatly appears at higher sintering temperature. The XRD revealed the changes in the crystal phase due to sintering temperature. SEM is a useful tool to follow structural changes that occur at the surface of ceramics.

Bondioli *et al.* [67] resulted from the research conducted on the possibility to use RHA as a silica precursor in ceramic materials, such as ceramic glazes were reported. The selected frits were prepared in a semi industrial furnace and the obtained glasses were investigated in comparison with the frits prepared from pure quartz. They concluded that RHA as a silica precursor can be used for the development of glazes for ceramic tile.

Ruangtanaweep *et al*. [68] have investigated the composition and phase of major biomasses fly ash in Thailand at different sintering temperatures. It has been found that, Rice husk ash, sugarcane leaves ash, straw ash and plam petiole ash at all sintering temperatures and bagasse ash at 800 and 1,000 ^{o}C have silica content of >50 wt. %, and they further found ashes were in SiO_2 form. The sintering temperature affected the purification and crystallization of the silicon composition in biomass samples. These results indicate that rice husk ash, Sugarcane leaves ash, and straw ash, palm petiole ash and bagasse ash may use substituted or additive for a silica source in the glass manufacturing process.

Dongmin *et al.* [69] worked to deal with the production of silica powders and active carbon from RHA with a consecutive method. The RHA is firstly treated with acid leaching to remove mineral composition, and then is boiled with a base to leach silica.

Liou *et al.* [70] studied that use of rice husk as a raw material to prepare nano-silica without adding an extra surfactant. The proposed method of preparing nano-silica from rice husk is simple and well suited to mass production, and helps minimize waste disposal problems.

Singh *et al*. [71] identified the characteristics of both the fly ash (FA) and rice husk ash using spectroscopic and microscopic analysis. SEM, XRD, XRF and FTIR spectroscopic methods were used for the characterization of treated and untreated ashes. The results were compared and it was observed that both ashes possess nearly same chemical phases and other functional groups thus proposing the use of rice husk ash as reinforcement like fly ash in Metal Matrix Composites (MMCs) specifically for wear resistance applications. XRF and XRD studies revealed the presence of almost similar elements in both untreated and treated FA and RHA powders. Hardest substances like SiO_2, Al_2O_3 were present as major constituents which can be used as particulate reinforcements in composites for wear-resistant applications. FTIR graphs showed that Quartz, Mullite and Vitereous phases were present in both powder and proposed to use RHA as particulate reinforcement in MMCs.

Amu *et al*. [72] determined the geotechnical properties of lateritic soil modified with sugarcane straw ash with a view to obtaining a cheaper and effective replacement for the conventional soil stabilizers. This result showed that sugarcane straw ash improved the Geotechnical properties of the soil samples. The optimum moisture content increased with increasing california bearing ratio (CBR) increased from 6.31 to 23.3 %, 6.24 to 14.88 % and 6.24 to 24.88 % and unconfined compression strength increased from 79.64 to 284.66 kN/m^2, 204.86 to 350.10 kN/m^2 and 240.4 to 564.6 kN/m^2 in samples A, B and C respectively. Sugarcane straw ash was therefore found as an effective stabilizer for lateritic soils.

Wasanapiarnpon *et al.* [73] investigated the effects of spodumene addition on densification, physical properties and thermal expansion coefficient, 25 and 50 mass % of spdumene were added to the mixture. Low thermal expansion coefficient of 2.70 x $10^{-6}/^{o}C$ was achieved with only the petalite phase detection. The effects of spodumene addition on the sintering properties of silica glass from rice husk ash have been investigated. They concluded that the RHA with 50 mass % addition of spodumene can be a candidate for use as silica glass raw materials.

Zerbino *et al*. [74] demonstrated that it is possible to produce structural concretes incorporating residual RHA ‘‘as nature’’ (NRHA), adapting the mixing process to optimize the ash particle size by grinding it in the mixer together with the coarse aggregate. This paper studies the development of alkali-silica reaction (ASR) in mortars and concretes prepared with NRHA and GRHA. Accelerated and long term expansion tests, mechanical characterization, microscopic observations and studies on prototypes are included. The RHA can inhibit or promote ASR depending on its particle size.

Tommy *et al*. [75] aimed at revealing the origin of high specific surface area and high pozzolanic activity of RHA by exploring its structure at micro and nano level. Rice husk calcined at 500, 600, 700 and 800 ^{o}C, was tested for compressive strength. The optimum combustion temperature for obtaining highly reactive RHA is 600 ^{o}C. Inner, outer interfacial with honeycombed pores was actually the main reason for very large specific surface area and very high chemical activity of RHA.

Andreola *et al.* [76] prepared glass-ceramic by using rice husk ash (RHA) as silica precursor. Glass-ceramic tiles were produced by a sinter-crystallization process using a glassy frit formulated in the $MgO\text{-}Al_2O_3\text{-}SiO_2$ composition system. The realized glass-ceramics were

studied according to ISO rules for sintering and technological properties (water absorption, apparent density, bending strength, Young's modulus, deep abrasion, Mohs hardness). Finally, chemical durability tests on parent glass and derived glass-ceramics were performed. The results obtained showed that it is possible to use RHA to produce glass-ceramic tiles by a sinter-crystallization process, obtaining Nepheline (Na_2O-Al_2O_3-SiO_2) as main crystalline phase and forsterite ($2MgO$-SiO_2) at 900 ^oC.

Tuscharoen *et al.* [77] reported on the structural optical and radiation shielding properties of development barium-borate-rice husk ash glasses (RHA) system. The glasses containing BaO in $xBaO:(80-x)B_2O_3$:20RHA where x = 45, 50, 55, 60, 65 and 70 wt.% have been prepared by melt quenching technique. The structural properties of these glasses are shown from density data and molar Volume. The mass attenuation of these glasses at photon energy 662 keV increasing too when BaO concentration increases. These data should be helpful in potential applications in gamma-ray shielding.

The applications rice husk ash (RHA) for property modification of high density polyethylene (HDPE) has been reported by **Ayswarya *et al.*** [78]. In this study RHA is blended with HDPE in the presence of a compatibilizer. The compatibilized HDPE-RHA blend has a tensile strength about 18 % higher than that of virgin HDPE. The elongation-at-break is also higher for the compatibilized blend. TGA studies reveal that uncompatibilized as well as compatibilized HDPE-RHA composites have excellent thermal stability. The results prove that RHA is a valuable reinforcing material for HDPE.

Behak *et al.* [79] studied that the behavior of amorphous silica was found in the RHA for incineration controlled temperatures up to 800 ^oC, meanwhile for 900 ^oC, the silica is rather crystalline. An upper limit temperature to reach a highly reactive RHA would be of 800 ^oC. For the purpose of stabilization of sandy soils, the optimum incineration temperature range of RHA is of 650-800 ^oC. The RHA would be of highest pozzolanic reactivity within this temperature range. The results showed that the optimal reactivity of the RHA is reached for a range of controlled temperature of 650-800 ^oC, providing a significant increase on the strength and stiffness of mixtures.

Mohamed *et al*. [80] investigated that the rice husk ash is well employed in the synthesis of zeolite particles (NaY and NaP). Physicochemical properties of the produced zeolite, after

optimizing the various synthesis conditions (24 h of crystallization time and 1100 ^{o}C) were characterized. SEM shows that NaY zeolite synthesized has a uniform distribution of particle size. The obtained data from particle size distribution showed homogeneity of zeolite Y. BET results revealed that, the BET surface area of the product from the one step route was lower than that of the two-step route because of the presence of zeolite P. In the two-step route, a longer crystallization time in this route resulted in a mixed phase containing NaY and zeolite P in sodium form (NaP). In addition, a one-step synthetic route (no aging) was studied and the product was zeolite P.

Xu *et al.* [81] were obtained the SiO_2 film with the water contact angle of 50.09 by sol-gel method using nano-rice husk ash prepared via burning rice-husk with self-propagating method. The super-hydrophobic SiO_2 films from nano-husk ash were prepared by sol-gel method using hydroxy silicone oil (HSO), hexa-methyldisilazane (HMS), or methyl triethoxysilane (MTS) as modifiers.

Olawale *et al.* [82] have prepared high purity silica by reflux raw rice husks (RRH) in oxalic acid which further removed the impurities, then burnt at 650 °C for 3 hours. The aim of this research is characterization of micro crystalline silicon production from rice husk ash. This silica was further used as a starting material for silicon (Si) preparation by metallothermal reduction process, using Mg as a reducing agent at 650 °C for 3 hours.

Based on literature summary, the rice husk ash and sugarcane leaves ash can used as initial ingredient in many applications particularly in glass industries. In the present study, we have taken both the components in different wt. (%) percent to make the different glass/ceramics are characterized by different techniques .the details of the characterizations are given in chapter 3 followed by results and discussion.

Chapter-3

Methodology and experimental procedure

This chapter describes the details of sample preparation, experimental procedure and characterization of different glasses/ceramics.

3.1 Sample preparation: Rice husk was obtained from a rice mill and sugar cane leaves were taken from a farm. Both were washed with water to remove adhering soil and dust and then it was burned in open air to convert into ash. These ash samples were labeled as R and S. Five samples with different weight percentage of rice husk ash (RHA) and sugarcane leaves ash (SCLA) were taken the sample labels along with compositions in wt % are given in **table 1.3.**

Table 3.1 Compositions by weight percentage and their labels.

Label	RS-1	RS-2	RS-3	RS-4	RS-5
RHA (wt %)	100	75	50	25	0
SCLA (wt %)	0	25	50	75	100

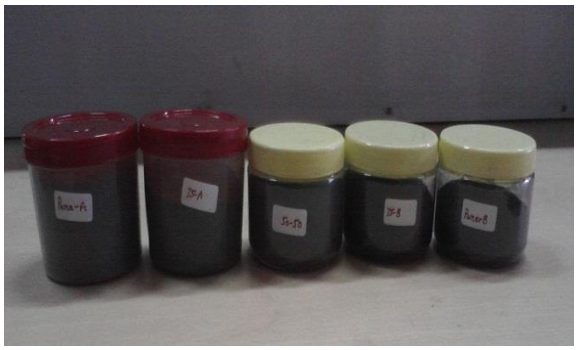

Figure 3.1 Prepared samples by mixing of RHA and SCLA.

Various mixtures were ground and mixed in an agate mortar - pestle for homogenization. The ground mixtures were calcinated at temperature 1000 ^{o}C in alumina crucible for 1.5 h. The calcined powders were again ground in an agate mortar pestle to get very fine powder. Pellets of these powders were prepared by adding varying small amount of binder poly-vinyl-alcohol (PVA). The powder palletized applying pressure is 12 KN/cm^2. The prepared pellets are having diameter and thickness was 20 mm and 5 mm respectively. After that these pellets were used for melting at 1550 ^{o}C with heating rate of 5 ^{o}C/ min.

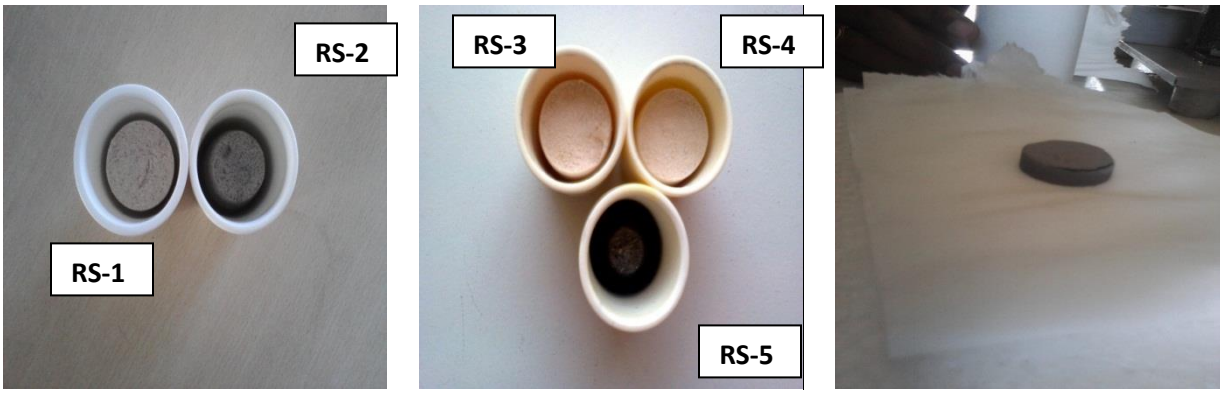

Figure 3.2 Calcined powder of RS-1,RS-2 RS-3, RS4 and RS-5 and Prepared pellet.

Figure 3.3 Molten mass in alumina crucible and glass sample.

Different characterization techniques were used to determine the different properties of prepared glass/ceramic samples**.** X-ray diffraction technique was used to confirm the amorphous nature of glass and further used to have information about the various phases present in the crystalline samples. XRD patterns of the samples were carried out on a PANalytical's X'Pert PRO MPD diffractrometer. During the experiment the wavelength of the incident X-ray was 1.54 Å with step size 0.013^{o} in 2θ range between $10\text{-}80^{o}$. Fourier Transform Infrared (FT-IR) transmission spectra of the samples were taken in the wavenumber range 400-1600 cm^{-1} on Perkin Elmer-Spectrum RX-1. Samples were prepared by taking 2 mg of glasses with KBr (200 mg) and mixed properly with agate mortar and compacted into 13 mm diameter pellets with 0.5 mm thickness. FTIR spectrometer was used to have a better understanding of the bonding between constituent atoms. Dilatometric measurement of all the samples was taken in order to calculate the linear thermal expansion coefficient (TEC), glass transition (Tg), softening point (Ts) and shrinkage etc. These measurements were done on NETZSCH (DIL 402 PC) from RT-800 ^{o}C in air at a

heating rate 5 ^{o}C/min. Both the surface of all glass samples was prepared smooth with the help of emery paper having the dimensions of the samples (1m×1m) with ~ 1.5 mm thickness. Thermo graphs have been taken between temperature and the percentage change in length of the samples. UV/visible absorption spectrums were recorded at room temperature in the range of 200-800 nm (ELICO 120 double beam spectrophotometer). The sample made as homogenous to eliminate any kind of interfaces by dissolving it in transparent solvent. The liquid contained in a vessel made a transparent material like silica corvette. UV-visible spectra of the samples were taken to calculate the optical band gap of the samples. The local structure changes in the glass and glass ceramic samples were examined by Raman spectroscopy. Raman spectra of the powder samples were collected using a Renishaw in Via Raman spectrometer with the 514.5 nm line of an Ar+ laser at 20 mW power. The instrument was calibrated using silicon as a reference at 520 cm^{-1} within ±1 cm^{-1}. Raman intensities to be recorded from 50-600 cm^{-1} shifted Raman region. A powder sample of the glass and glass ceramic was loaded into a plastic sample holder. The surface was made flat by compressing the powder. Spectra were taken from various locations on the samples to examine the homogeneity in the samples

The detail description about the characterization techniques is given below:

3.2 X-ray Diffraction (XRD)

The atomic planes of a crystal cause an incident beam of X-rays to interfere with one another as they leave the crystal. The phenomenon is called X-ray diffraction.

X-ray diffraction is a rapid analytical technique primarily used for phase identification of a crystalline material and can provide information on unit cell dimensions as well as their volume fraction crystallite size and strain present in lattice.

3.2.1 Principle

X-ray diffraction is based on constructive interference of monochromatic x-rays & crystalline sample. X-rays are generated by a cathode ray tube, filtered to produce monochromatic radiation, collimated to concentrate & directed toward the sample. The interaction of incident rays with the sample produces constructive interference when conditions satisfy the Bragg's law. All diffraction method is based on the generation of X-rays.

Figure 3.4 Photograph of X-ray diffraction [83].

Bragg's law:

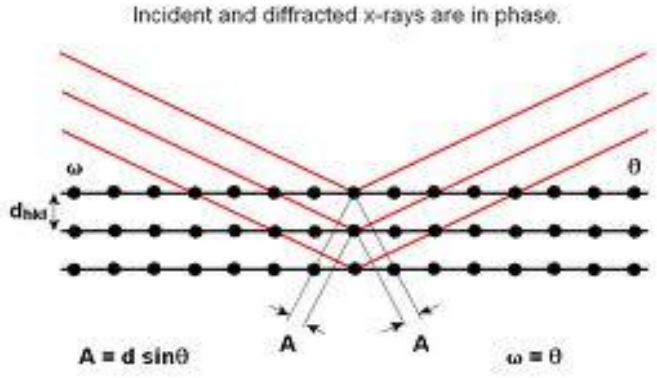

Figure 3.5 Schematic diagram of X-ray scattering.

When a crystal is bombarded with x-rays of a fixed wavelength and at certain incident angles, intense reflected x-rays are produced when the wavelength of the scattered X-rays interferes constructively. In order for the wave of interfering constructively, the differences in the travel

path must be equal to integral multiples of the wavelength. When this constructive interference occurs, a diffracted beam of X-rays will leave the crystal at an angle equal to that of the incident beam. To illustrate this feature, consider a crystal with crystal lattice planer distances d, where the travel path length differences between the ray paths of two beams is an integer multiple of the wavelength, constructive interference will occur for a combination of that specific wavelength, crystal lattice planer spacing and angle of incidence (θ). Each rational plane of atoms in a crystal is a single unique angle. The general relationship between the wavelengths of the incident X-rays, angle of incidence and spacing between the crystal lattice planes of atoms is known as Bragg's law:

$$\mathbf{2\ d\ \sin\theta = n\lambda}$$

Where n is an integer that indicates the order of diffraction, λ is wavelength of the incident x-rays, d is the inter-planar spacing of the crystal and θ is angle of incidence. The following information can be achieved by X-ray diffraction.

- Degree of crystallinity
- crystalline phase, and crystal structure
- Crystallite size from analysis of peak broadening
- Crystallite shape from study of peak symmetry

3.3 FTIR (Fourier Transform Infrared spectroscopy)

FTIR is the most useful technique for identifying organic or inorganic chemicals. FTIR can be applied to the analysis of solids, liquids, and gasses. Today's FTIR instruments are computerized which makes them faster and more sensitive than the older dispersive instruments.

FTIR stands for Fourier Transform Infrared, the preferred method of infrared spectroscopy. In infrared spectroscopy, IR radiation is passed through a sample. Some of the infrared radiation is absorbed by the sample and some of it is passed through (transmitted). The resulting spectrum represents the molecular absorption and transmission, creating a molecular fingerprint of the sample. Like a fingerprint no two unique molecular structures produce the same infrared spectrum. An infrared spectrum represents a fingerprint of a sample with absorption peaks which correspond to the frequencies of vibrations between the bonds of the atoms making up the

material. Each different material is a unique combination of atoms therefore no two compounds produces the exact same infrared spectrum.

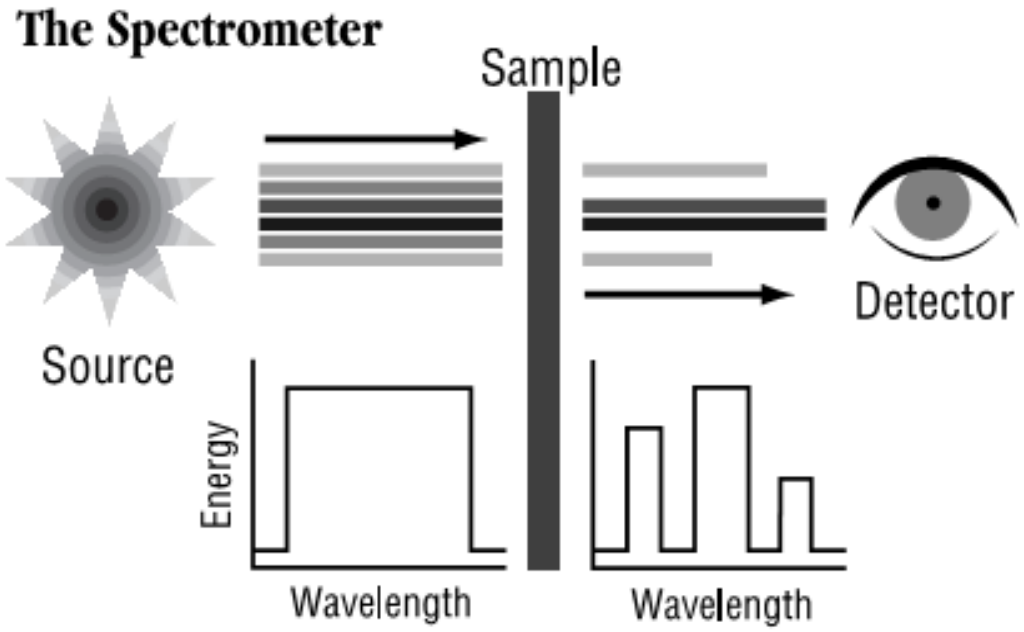

Figure 3.6 Schematic diagram of X-ray diffraction spectrum [83].

Therefore, infrared spectroscopy can result in a positive identification (qualitative analysis) of every different kind of material. In addition, the size of the peaks in the spectrum is a direct indication of the amount of material present.

Fourier transform infrared spectroscopy is preferred over dispersive or filter methods of infrared spectral analysis for several reasons:

a) It is a non-destructive technique.
b) It provides a precise measurement method which requires no external calibration.
c) It can increase speed, collecting a scan every second.
d) It can increase sensitivity-one second scans can be co-added together to ratio out random noise.
e) It is mechanically simple with only one moving part.

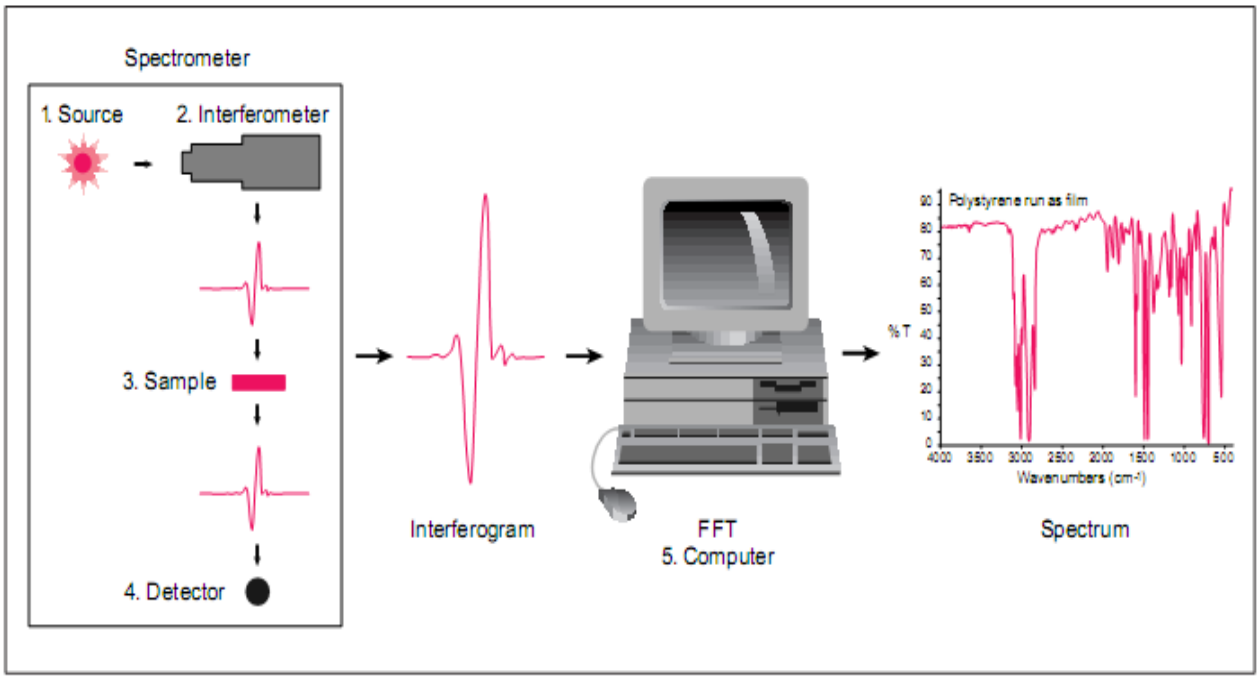

Figure 3.7 Computer interfaced spectrometer and spectrum.

3.3.1 Applications of FTIR Spectroscopy

- To Organic compounds
- Structure of many inorganic compounds
- De-formulations
- Forensics
- Material homogeneity

3.4 Ultraviolet–visible spectroscopy

Ultraviolet–visible spectroscopy or ultraviolet-visible spectrophotometry (UV-Vis or UV/Vis) refers to absorption spectroscopy or reflectance spectroscopy in the ultraviolet-visible spectral region. This means it uses light in the visible and adjacent (near-UV and near-infrared (NIR)) ranges. The absorption or reflectance in the visible range directly affects the perceived color of the chemicals involved. In this region of the electromagnetic spectrum, the molecules undergo electronic transitions. If a sample of unknown compound is exposed to light, certain functional group within the molecules absorb UV light different wavelengths.

3.4.1 Origin of UV-VIS Spectrum

The absorption of radiation in the UV-VIS region of the spectrum is dependent on the electronic structure of the absorbing species, like atoms, molecules, ions or complexes. The absorption spectrum of atomic species consists of a number of narrow lines that arise as a consequence of the transition amongst the atomic energy levels. In molecules, the electronic, vibrational as well as the rotational energies are quantized. A given electronic energy level has a number of vibrational energy levels in it and each of the vibrational energy level has a number of rotational energy levels in it. When a photon of a given wavelength interacts with the molecule it may cause a transition amongst the electronic energy levels if its energy matches with the difference in the energies of these levels. In the course of such transitions, for the sample in gaseous or vapor phase, the spectrum consists of a number of closely spaced lines constituting what is called a band spectrum. However, in the solution phase, the absorbing species are surrounded by solvent molecules and undergo constant collisions with them. These collisions and the interactions among the absorbing species and the solvent molecules cause the energies of the quantum states to spread out. As a consequence, the sample absorbs photons spread over a range of wavelength. Thereby, the spectrum acquires the shape of a smooth and continuous absorption peak in the solution phase.

3.4.2 Characteristics of UV-VIS Spectrum

In order to obtain a UV-VIS spectrum the sample is ideally irradiated with the electromagnetic radiation varied over a range of wavelength. A monochromatic radiation i.e., a radiation of a single wavelength is employed at a time. This process is called scanning. The amount of the radiation absorbed at each wavelength is measured and plotted against the wavelength to obtain the spectrum. The UV spectra of substances are characterized by two major parameters, namely, the position of the maximum of the absorption band called λ_{max}, and the intensity of the bands. The λ_{max} refers to the wavelength of the most absorbed radiation and is a measure of the difference in the electronic energy levels involved in the transition. The intensity on the other hand is indicative of the probability of the transition i.e., whether the transition is allowed or not. It is also is a measure of the concentration of the absorbing species.

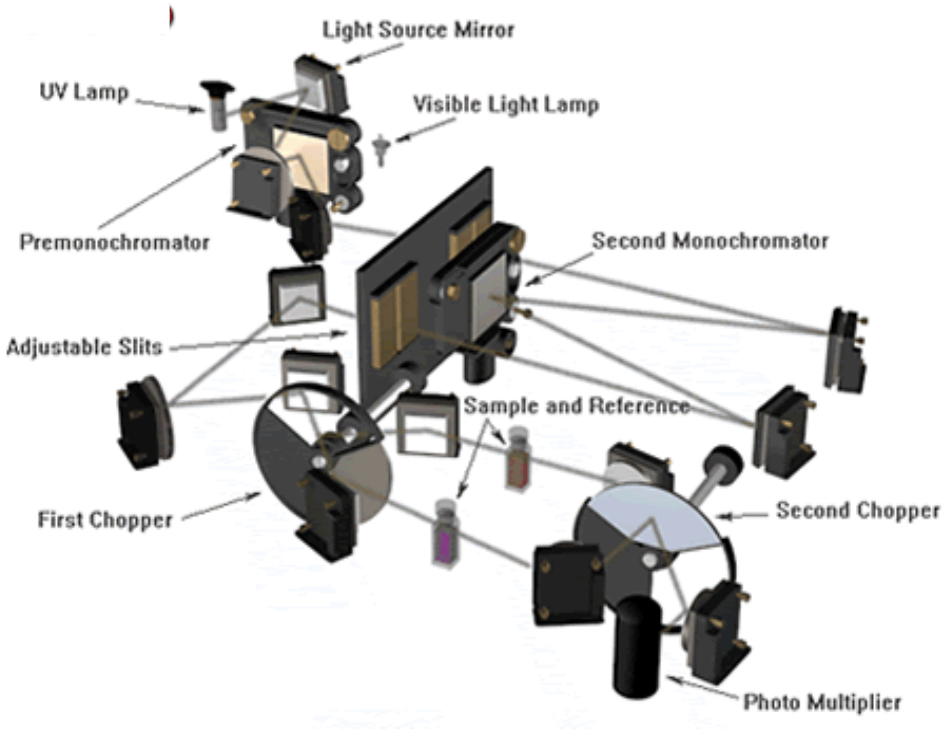

Figure 3.8 Schematic diagram of UV/Visible spectroscopy [84].

The characteristics of UV-VIS spectrum depend on the structure and concentration of the absorbing species in solution. Therefore, these spectra are extensively used in the characterization and in the quantitative estimations of the analytic. Broadly, following qualities can be evaluated using UV/Visible spectroscopy. Such that optical band gap, urbach energy, refractive index and optical basicity.

3.5 Dilatometry

3.5.1 Introduction

Dilatometry (DIL) is a thermo-analytical technique for the measurement of expansion or shrinkage of a material. Every material expands or contracts in response to heating or cooling. This response to temperature change is expressed as its coefficient of thermal expansion.

The coefficient of linear thermal expansion (CTE) is defined as:

$$\alpha = \frac{\left(\frac{dL}{L_o}\right)}{dT}$$

Here L_o is the initial length of the material, dL is the change in length and dT is the change in temperature. CTE is an important engineering parameter.

3.5.2 Principle

When a material is heated, we are giving energy to it. Atoms of the material start vibrating about their mean positions. As a net result, material expands. Its expansion is dependent on the types of bonding involved, strength of the material etc. In dilatometery, the thermal expansion of the material is measured as a function of temperature or time. A pushrod is connected to an inductive displacement transducer on one side. And on other, it is in close contact with a sample in order to register any length change in sample material during heating or cooling. Since the sample holder and the anterior part of the pushrod are exposed to the same temperature program as the sample, they also undergo expansion. The resulting dilatometer signal is therefore the sum of lengths changes of the sample, sample holder and pushrod. To obtain the true sample behavior, it is thus necessary to correct the raw dilatometer data. There are two possible correction methods: to use tabulated expansion data for the sample holder material or to use a correction curve – the latter of which is often more precise.

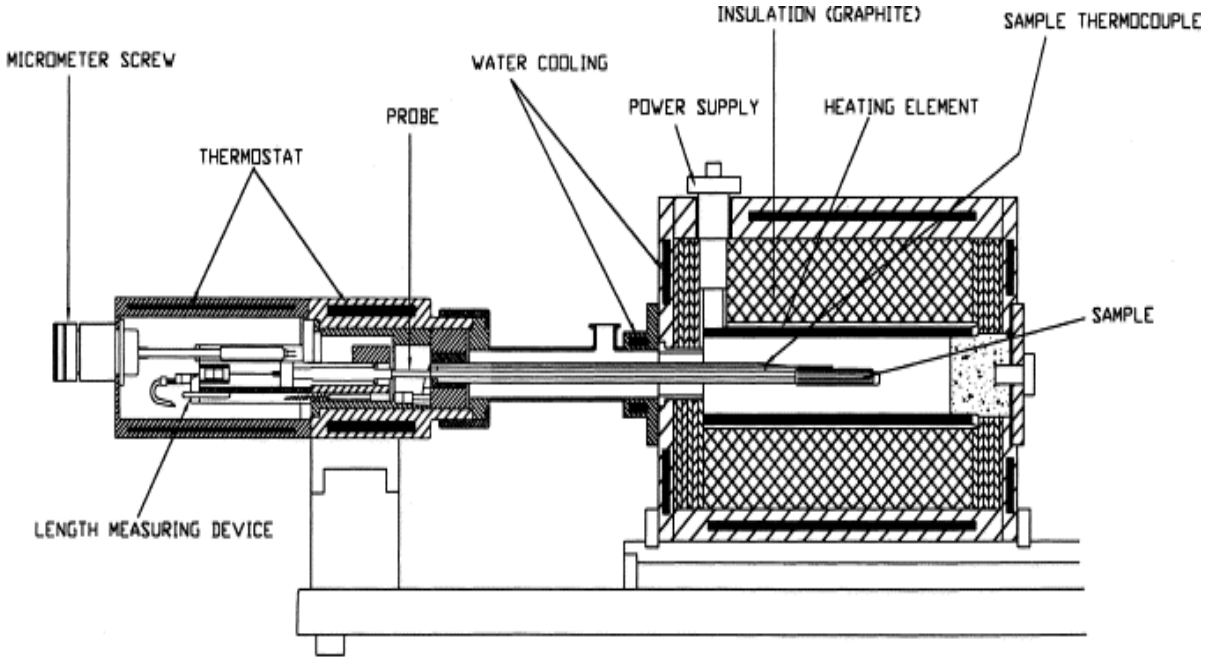

Figure 3.9 Schematic diagram of dilatometer [85].

The dilatometer is very important tool to know that the thermal expansion coefficient. Apart from this, we can also determine the glass transition temperature (Tg), phase transition and change in the density. Moreover, it can also be very use full techniques to find out the shrinkage and porosity of the samples.

3.6 Raman spectroscopy

Raman spectroscopy is a technique based on inelastic scattering of monochromatic light, usually from a laser source. Inelastic scattering means that the frequency of photons in monochromatic light changes upon interaction with a sample. Photons of the laser light are absorbed by the sample and then re-emitted. Frequency of the re-emitted photons is shifted up or down in comparison with original monochromatic frequency, which is called the Raman's effect. This shift provides information about vibrational, rotational and other low frequency transitions in molecules. Raman spectroscopy can be used to study solid, liquid and gaseous samples.

3.6.1. Origins of Raman Sparta

The Raman effect is based on molecular deformations in electric field E determined by molecular polarizability α. The laser beam can be considered as an oscillating electromagnetic wave with electrical vector E. Upon interaction with the sample it induces electric dipole moment $P = \alpha E$ which deforms molecules. Because of periodical deformation, molecules start vibrating with characteristic frequency υ_m. Amplitude of vibration is called a nuclear displacement. In other words, monochromatic laser light with frequency υ_0 excites molecules and transforms them into oscillating dipoles. Such oscillating dipoles emit light of three different frequencies when:

1. A molecule with no Raman-active modes absorbs a photon with the frequency ν_o. The excited molecule returns back to the same basic vibrational state and emits light with the same frequency υ_0 as an excitation source. This type if interaction is called an elastic Rayleigh scattering.
2. A photon with frequency ν_o is absorbed by Raman-active molecule which at the time of interaction is in the basic vibrational state. Part of the photon's energy is transferred to the Raman-active mode with frequency υ_m and the resulting frequency of scattered light is reduced to υ_0- υm. This Raman frequency is called Stokes frequency, or just **"Stokes".**

3. A photon with frequency υ_0 is absorbed by a Raman-active molecule, which, at the time of interaction, is already in the excited vibrational state. Excessive energy of excited Raman active mode is released, molecule returns to the basic vibrational state and the resulting frequency of scattered light goes up to $\nu_o + \nu_m$. This Raman frequency is called Anti-Stokes frequency, or just **"Anti-Stokes".**

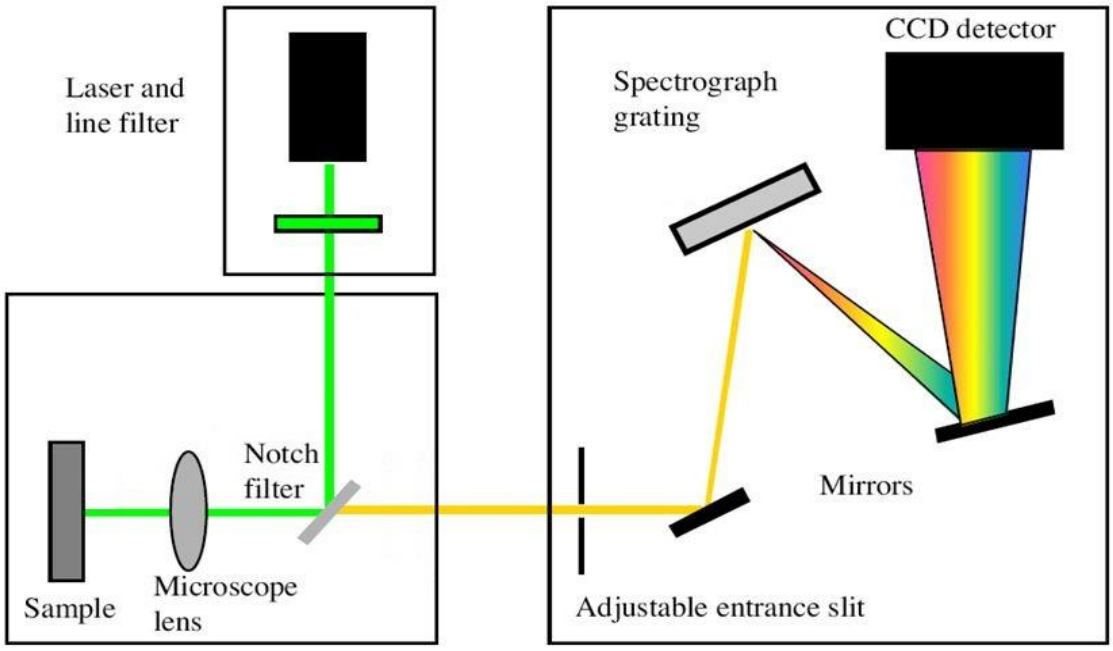

Figure 3.10 Schematic diagram of Raman spectroscopy.

About 99.999 % of all incident photons in spontaneous Raman undergo elastic Rayleigh scattering. This type of signal is useless for practical purposes of molecular characterization. Only about 0.001 % of the incident light produces inelastic Raman signal with frequencies $\upsilon_0 + \upsilon_m$. Spontaneous Raman scattering is very weak and special measures should be taken to distinguish it from the predominant Rayleigh scattering. Instruments such as notch filters, tunable filters, laser stop apertures, double and triple spectrometric systems are used to reduce Rayleigh scattering and obtain high-quality Raman

.

The Raman spectroscopy is very important tool of characterization particular carbon nano tubes are addition to conventional characterization of polymer and organic and inorganic materials.

Chapter-4

Results and discussion

4.1 X-ray diffraction

XRD spectra of all the prepared samples RS-1, RS-2, RS-3, RS-4 and RS-5 are shown in figures (4.1-4.5). The RS-1 and RS-2 samples exhibit sharp crystalline peaks. Whereas, RS-3, RS-4 and RS-5 samples show broad hump which indicate it is amorphous in nature. The XRD peaks of RS-1 and RS-2 samples are indexed with cristobalite phase (ICDD No. 01-076-0936), tridymite phase (ICDD No. 01-086-0680) and K_2O (ICDD No. 01-077-2151). The volume fractions of crystobalite, trydemite, and K_2O 60, 37and 3% respectively in RS-1 sample. These phases in RS-2 sample are 55, 44 and 5 %, respectively. The volume fraction of these phases depends on the initial contents of ash. As the content of sugarcane leave ash increase the crystalline phase particularly crystobalite decrease. As indicated in the table 1.3 and 1.4 the SiO_2 content is less in sugarcane leave ash as compared to rice husk ash.

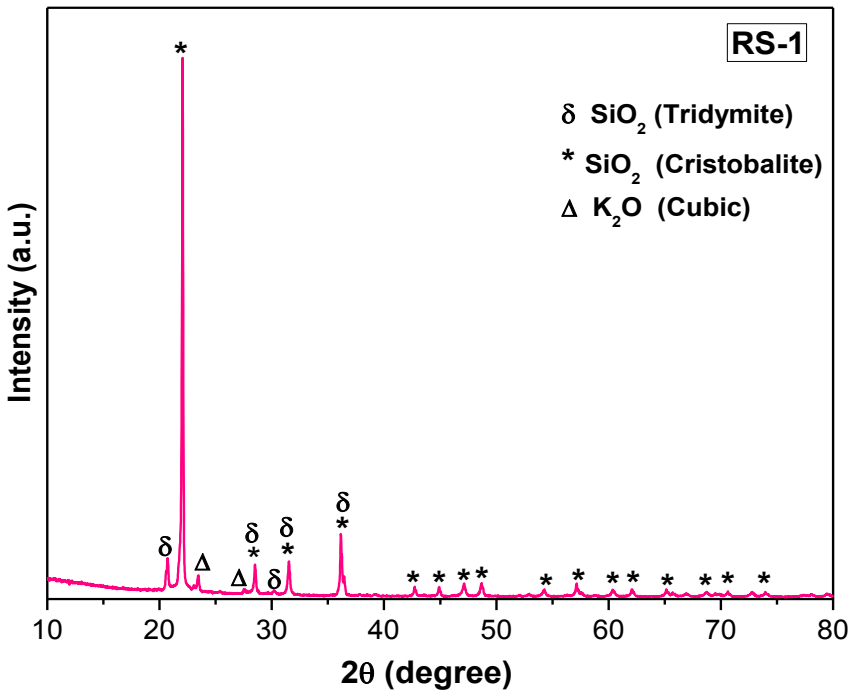

Figure 4.1 XRD pattern of RS-1 sample.

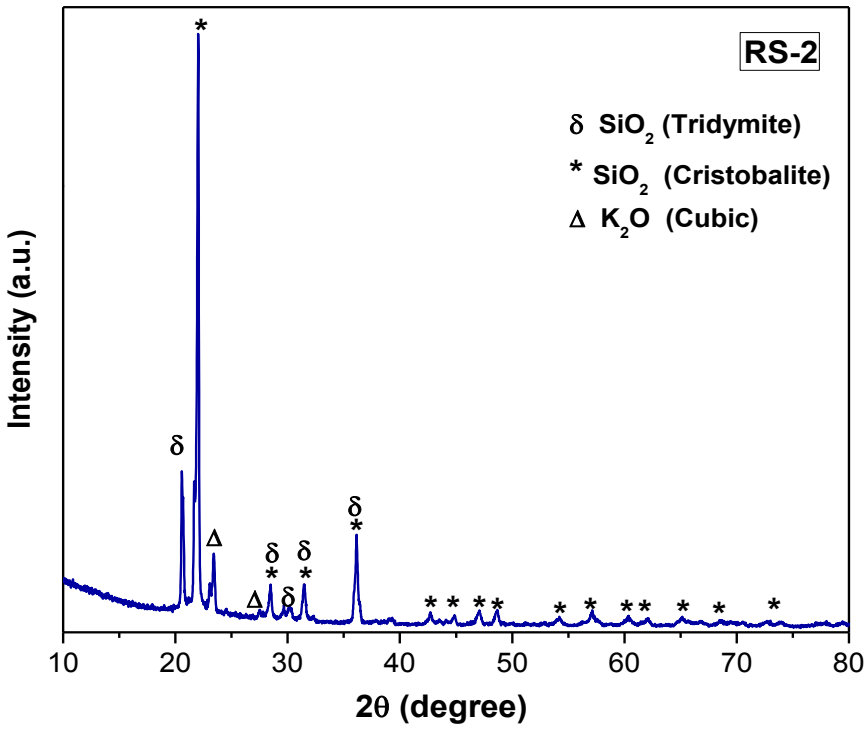

Figure 4.2 XRD pattern of RS-2 sample.

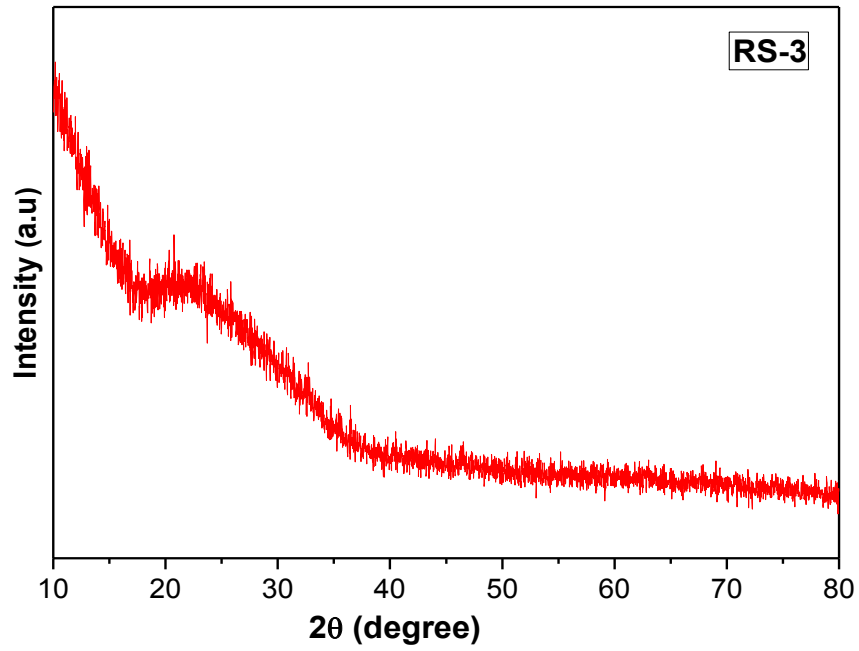

Figure 4.3 XRD pattern of RS-3 sample.

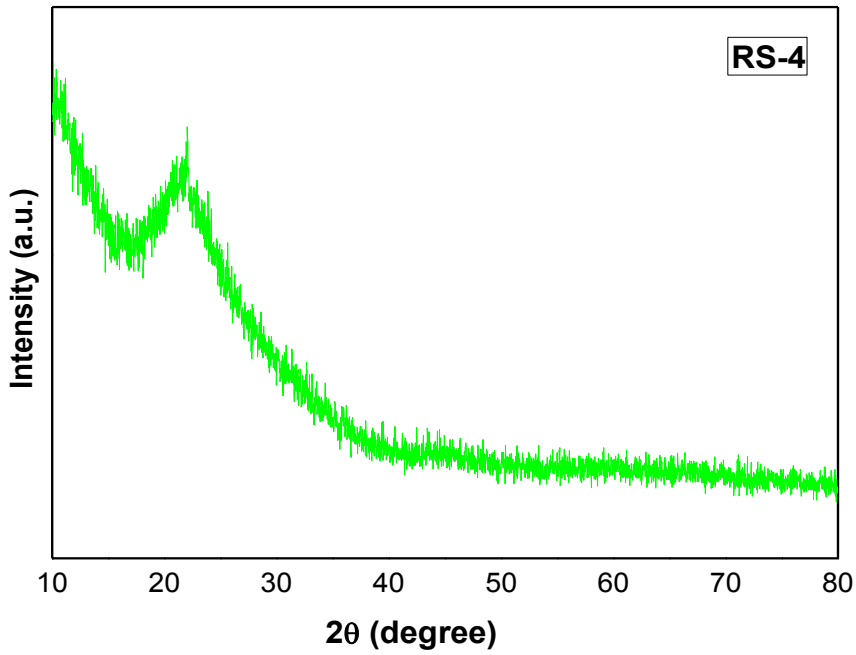

Figure 4.4 XRD pattern of RS-4 sample.

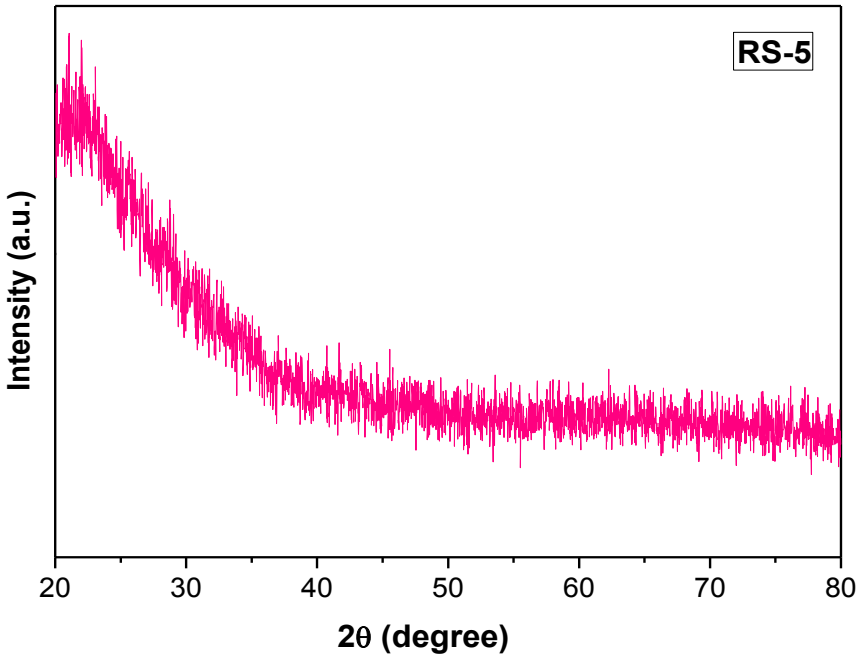

Figure 4.5 XRD pattern of RS-5 sample.

Obliviously the melting point of RS-2 will decrease with deceasing SiO_2 content. Moreover, the modifier CaO, MgO etc.is also higher in RS-2 sample [45]. As the sugarcane leave ash increase increases the crystalline phase disappeared and the sample becomes completely amorphous. These phenomena can also be explained on the base of higher contents of modifiers in RS-3 to RS-5 samples. Interestingly the RS-5 samples showed very high thermal stress since during the melting in the Al_2O_3 crucible was broken.

4.2 Dilatometeric study

Figure 4.6 shows the dilatometric curve for RS-1, RS-2 and RS-3 samples. RS-3 sample indicates almost linear behavior from room temperature to 500 ^oC. On the other hand, RS-1 and RS-2 sample shows a phase transition ~ 215 ^oC. This phase transition ~ 215 ^oC may be related to cristobalite, a high temperature phase of silica, SiO_2, undergoes a (meta-stable) first-order phase transition from a cubic to a tetragonal structure [86]. In addition to this, a second phase transition ~ 400 ^oC for RS-1 sample is also observed which is due to monoclinic to hexagonal phase transition of trymedite (a form of SiO_2) [87]. The double differentiation was done to get another clear picture for any other phase transition .A typical double differentiation of RS-3 is shown in figure 4.7. A clear cut phase transition is observed at 410 ^oC as evident in figure 4.7. This phase transition is in well agreement of RS-1. The thermal expansion coefficients (TEC) from 100-500 ^oC for samples RS-1, RS-2 and RS-3 are found to be 8.35, 9.64, 8.50 × 10^{-6}/^oC, respectively. The thermal expansion is related to the asymmetric potential well dependent on the bond nature and strength. RS-2 sample exhibits higher TEC than other two samples. It may be ascribed due to lower volume fraction of SiO_2 (Crystabolite phase) which exhibit low thermal expansion with large volume change with respect to temperature. The thermal expansion coefficient of RS-4 and RS-5 could not measure due to presence of very high stress and samples were broken in very small pieces.

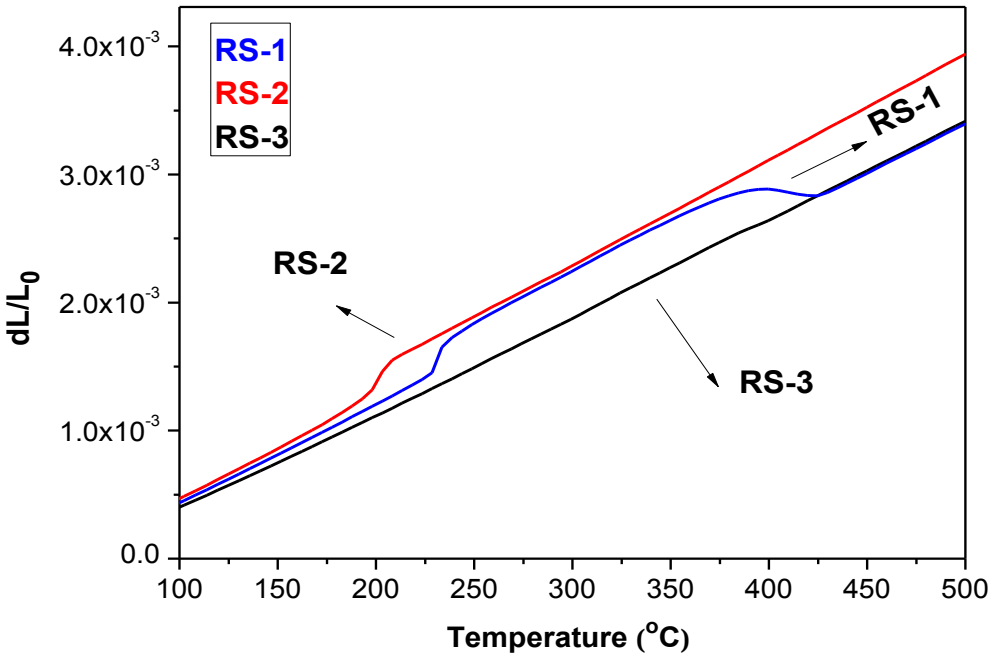

Figure 4.6 Dilatometric curves for RS-1, RS-2 and RS-3 samples.

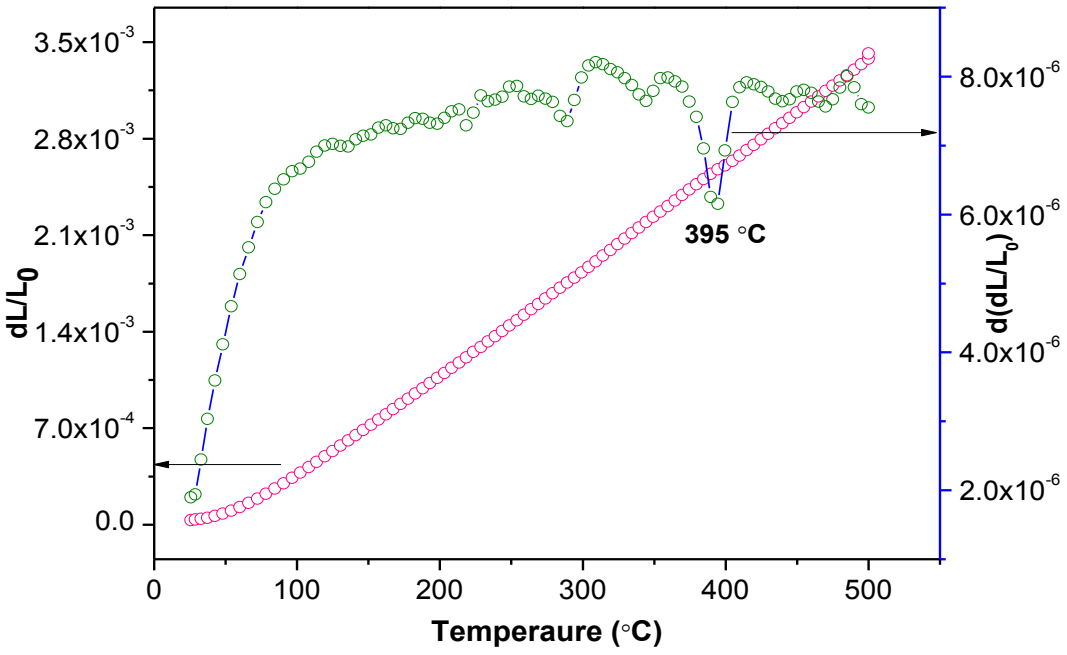

Figure 4.7 Double differentiation curve of RS-3 sample.

4.3 UV-Visible study

Figures (4.8-4.12) show the energy band gap curves for RS-1, RS-2, RS-3, RS-4 and RS-5 samples. The band gaps for RS-1 to RS-4 samples are found to be in the range of 4.5-5.0 eV. On the other hand, the energy band gap for RS-5 sample is found to be in the range of 3.0-6.0 eV. The optical band gaps in glasses broadly depend on the initial constituents. As modifier contents increase the non-bridging oxygen (NBO) also increase in the glasses which leads to decrease the band gaps in the glasses. Therefore, in case of RS-1, RS-2 and RS-3 samples the presence of NBO's is more led to lower band gaps. On the other hand RS-1 and RS-2 both are crystalline having different volume fraction of the phase it might be possible that the high volume fraction of K_2O phase may decrease the band gaps. All graphs exhibit two absorption region probably raised due to phase separation between these samples.

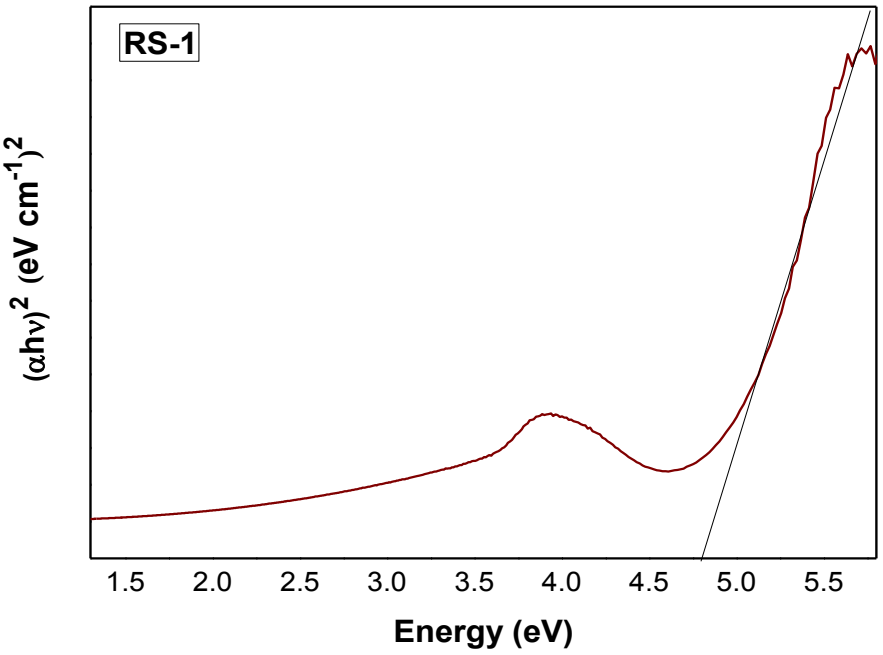

Figure 4.8 Energy band gap for RS-1 sample.

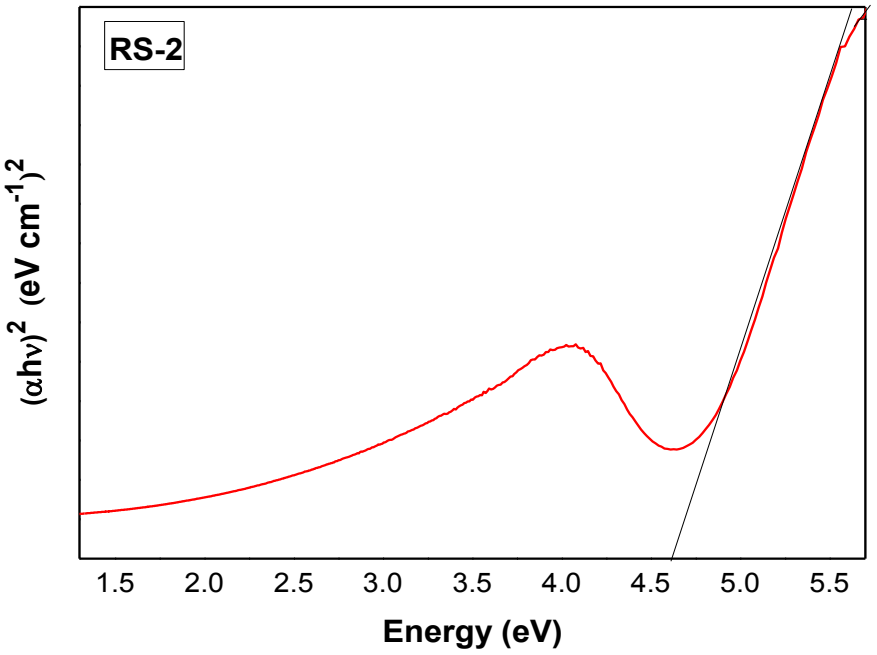

Figure 4.9 Energy band gap for RS-2 sample.

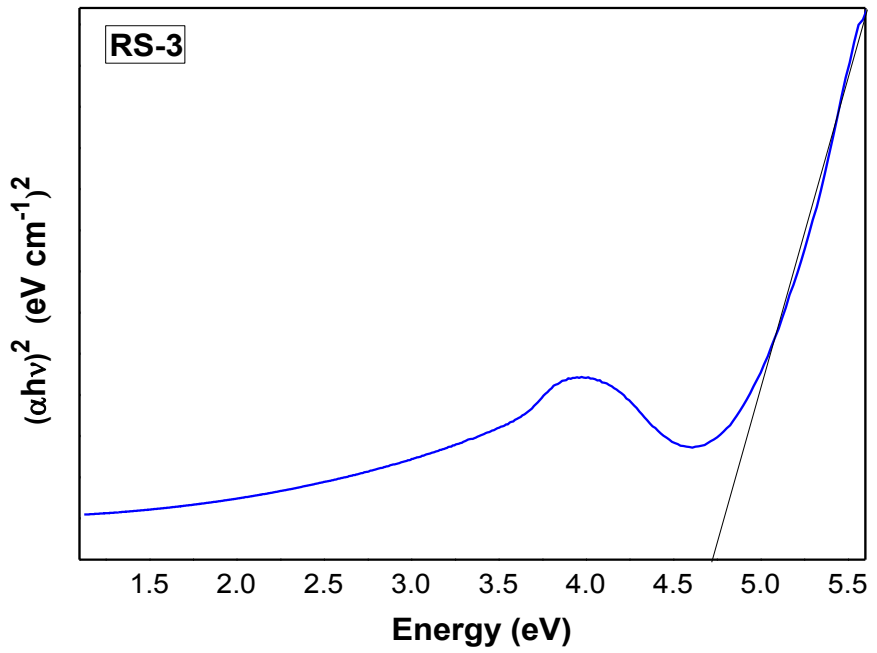

Figure 4.10 Energy band gap for RS-3 sample.

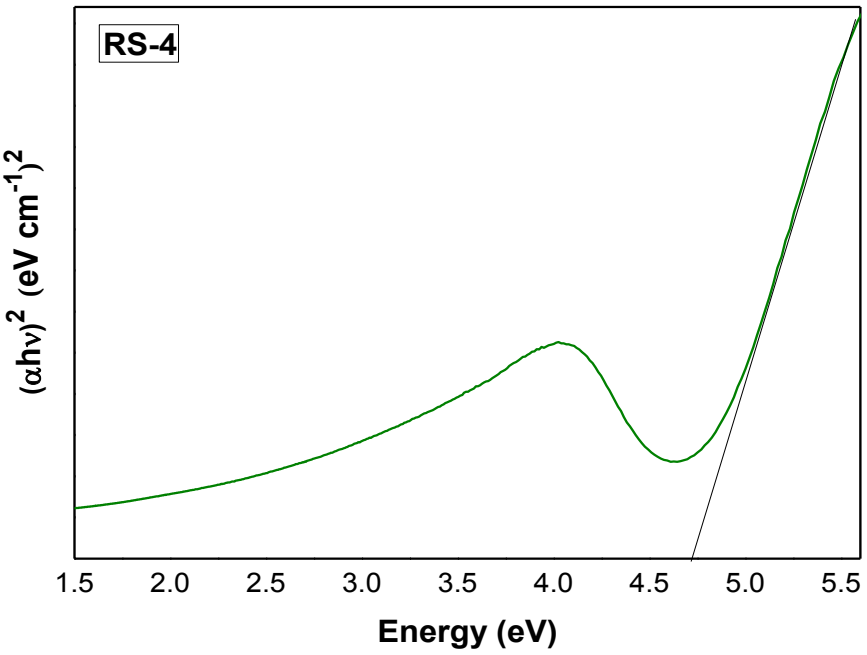

Figure 4.11 Energy band gap for RS-4 sample.

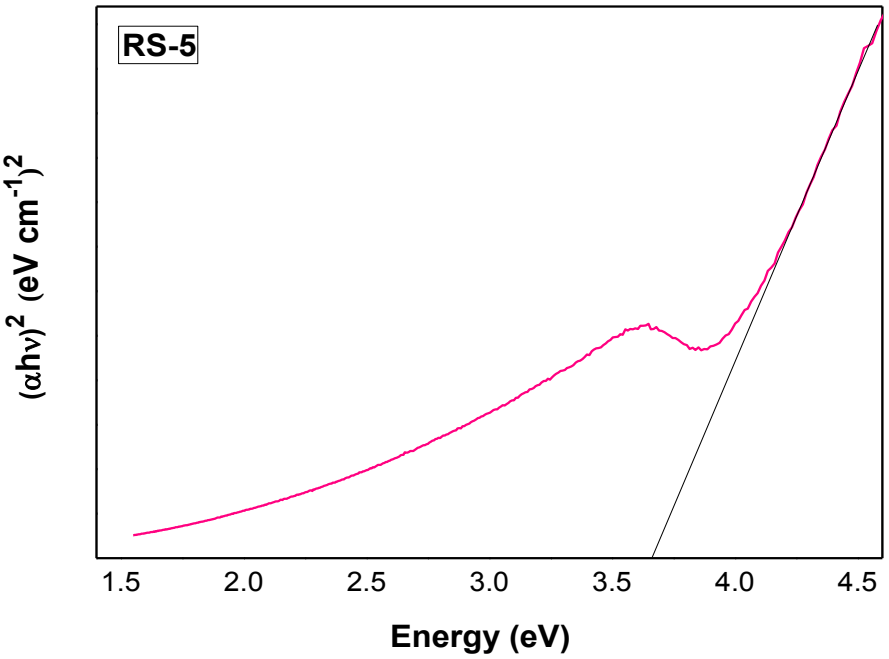

Figure 4.12 Energy band gap for RS-5 sample.

4.4 Fourier Transform Infrared analysis

The infrared absorption spectra of the samples have been recorded in order to obtain information about the possible changes of vibrational spectra due to the process of structural rearrangement with the change in glass composition**.** Figure 4.13 shows the FT-IR spectra for all glass and ceramic samples recorded in the range (400-1500 cm^{-1}). In figure 4.13 the glass samples RS-3, RS-4 and RS-5 shows mainly two bands at 471 and 793 cm^{-1}. On the other hand, ceramic samples RS-1 and RS-2 shows mainly three bands ~ 494, 624 and 793 cm^{-1}. In the case of glass ceramics band at 471 cm^{-1} is almost disappeared as compared to glass samples. The bands at 471 cm^{-1} and 624 cm^{-1} are attributed due to Si-O-Si bending vibrations and symmetric stretching vibration of Si-O, respectively [65, 81]. The weak band ~ 494 cm^{-1} is designate to ν_2 symmetric bending of the SO_4^{2-} tetrahedral group [88]. Moreover, the band at 793 cm^{-1} is assigned to the Si-O-Si symmetric stretching [89]. A broad transmittance band at around ~1100 cm^{-1} is common for all the samples and is attributed due to the asymmetric stretching vibrations of the Si-O-Si bonds [90]. The ceramic samples have very sharp bands as compared to glass samples. Obviously, the sharpness of bands also related to the bond strength. The crystalline (RS-1 and RS-2) samples have well defined bonds having uniform frequency vibrations.

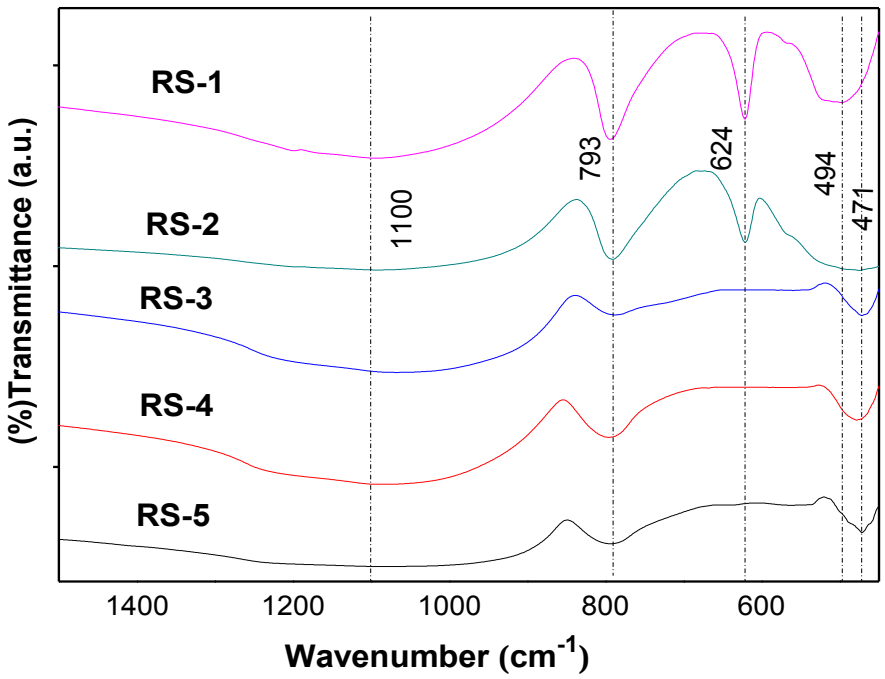

Figure 4.13 FTIR spectra for RS-1, RS-2, RS-3, RS-4 and RS-5 samples.

4.5 Raman Spectroscopy analysis

Figures (4.14 - 4.18) show the Raman spectra for RS-1, RS-2, RS-3, RS-4 and RS-5 samples. Raman spectra mainly show four bands for RS-1 and RS-2 samples ~ 114, 232, 289 and 420 cm^{-1}, respectively. On the other hand, RS-3 sample show very weak three bands ~ 148, 284 and 453 cm^{-1}. With increase of sugarcane content in RHA the Raman bands ~ 284 and 453 cm^{-1} for RS-4 and RS-5 samples almost disappeared shown in figures 4.17 and 4.18, respectively. The bands ~ 114, 232 and 420 cm^{-1} are attributed due to symmetric stretching of Si-O-Si bond in cristobalite (SiO_2) phase [91]. The bands in the range of (284-298 cm^{-1}), 369 cm^{-1} and ~ 458 cm^{-1} are designates to O-Si-O bending vibrations [92]. These results are also confirmed by FT-IR results of similar samples. Furthermore, more details study is required with wider frequency range to confirm the Raman Shift in the present samples.

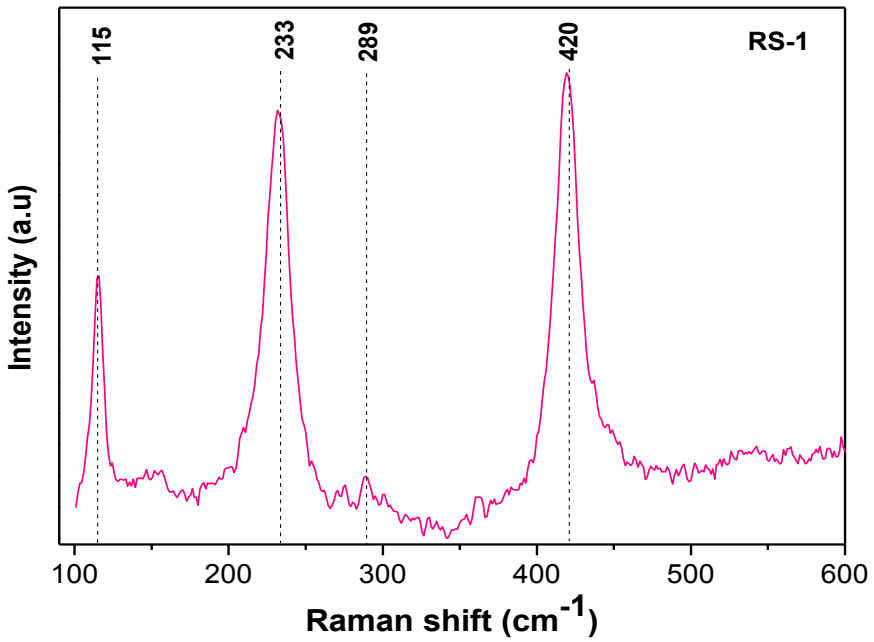

Figure 4.14 Raman spectra of RS-1 sample.

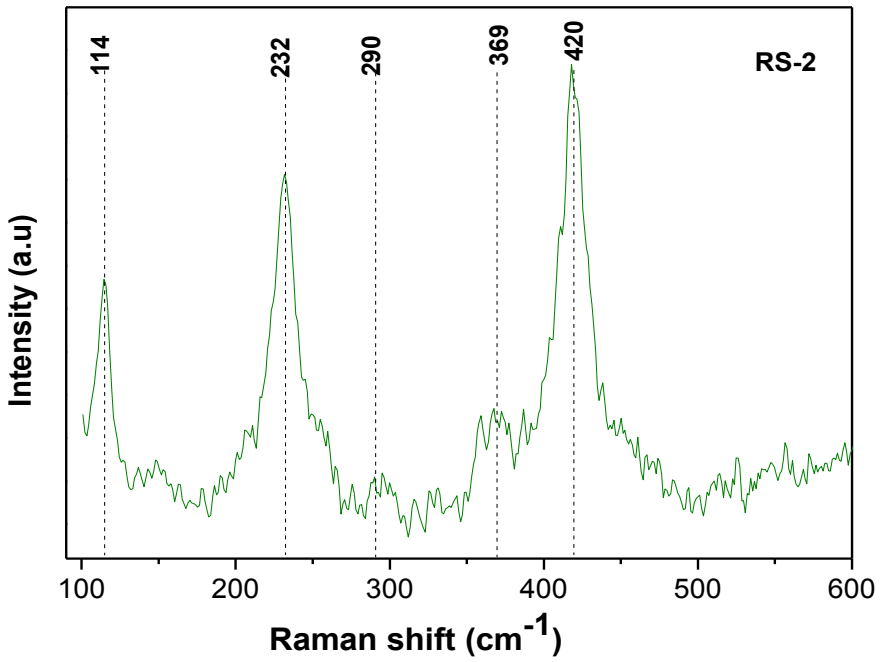

Figure 4.15 Raman spectra of RS-2 sample.

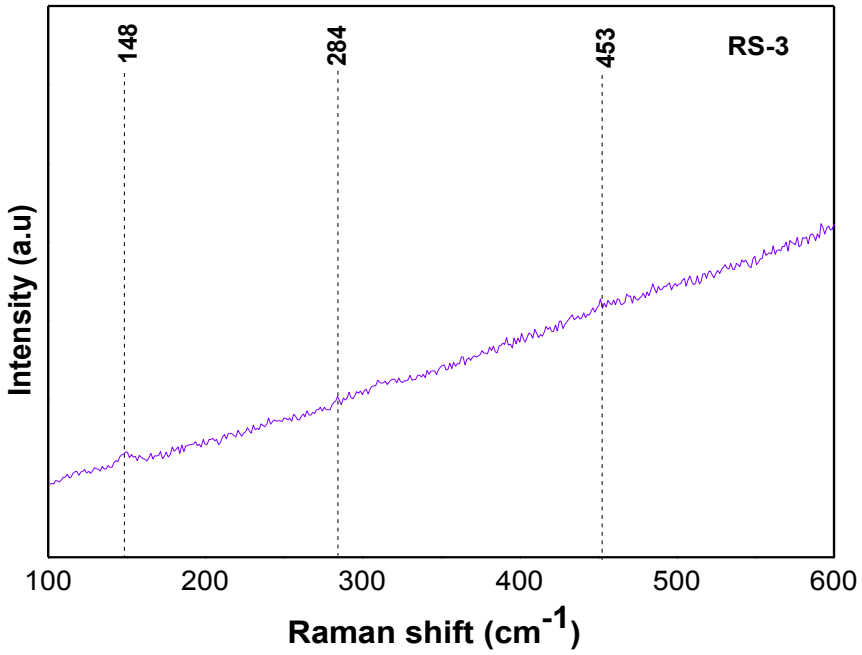

Figure 4.16 Raman spectra of RS-3 sample.

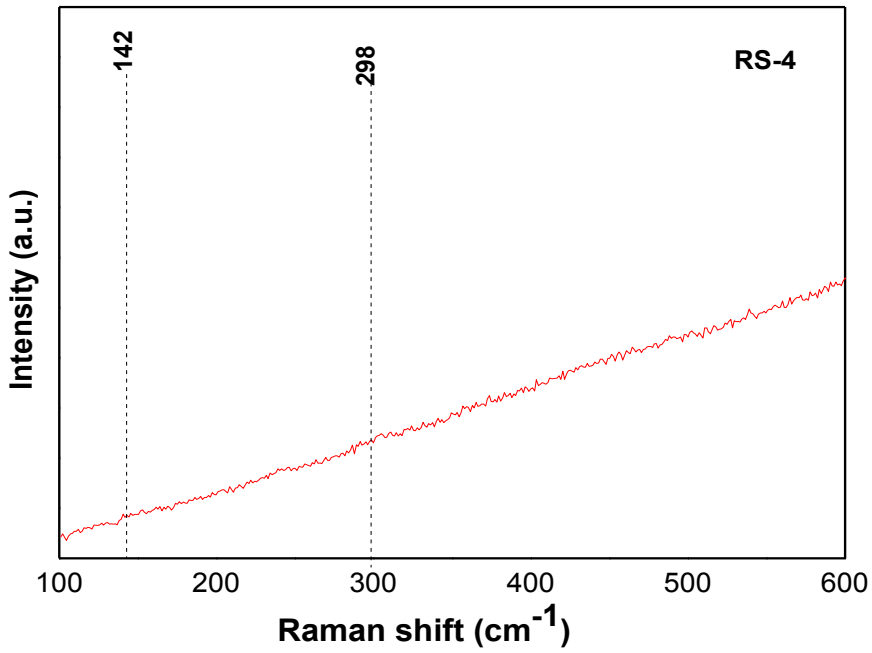

Figure 4.17 Raman spectra of RS-4 sample.

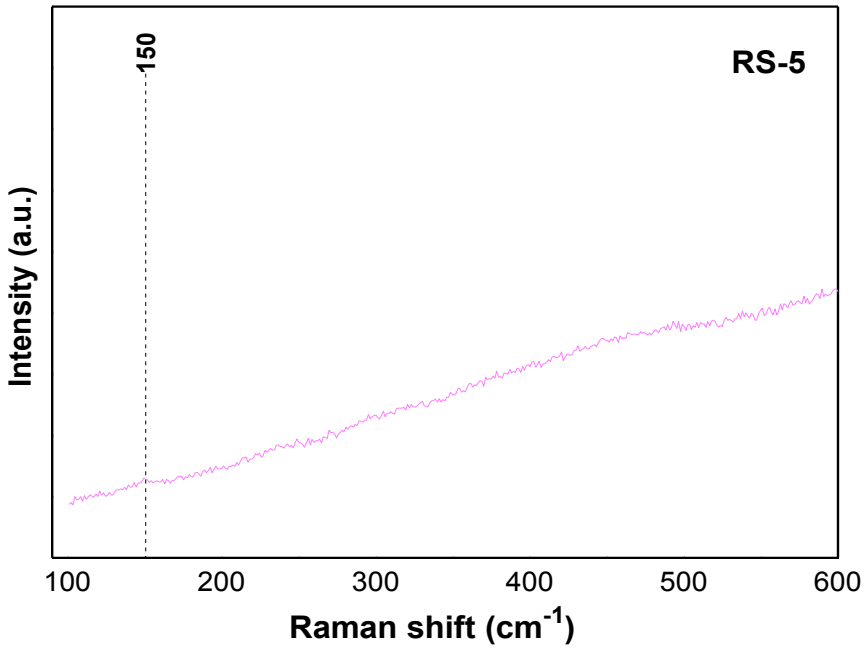

Figure 4.18 Raman spectra of RS-5 sample.

Chapter 5

Conclusions

Rice husk ash (RS-1) samples show the presence of crystalline phase. The addition of sugarcane leaves ash decreases the crystalinity in the present samples. These crystalline phases were indexed with cristobalite phase of crystalline silica, tridymite phase of crystalline silica, and K_2O phase. The volume fractions of these phases in RS-1 sample are 60, 37 and 3 % respectively. Whereas, the volume fractions of these phases in RS-2 sample are 55, 40 and 5 % respectively. Dilatometric study reveals two phase transitions ~ 215 ^oC and ~ 400 ^oC. The phase transition ~ 215 ^oC ascribed due to cristobalite, a cubic to a tetragonal structure. Moreover, the phase transition ~ 400 ^oC occurred due to monoclinic to hexagonal phase transition of trymedite (a form of SiO_2). Band gap found to be in the range of 3.5-4.5 eV of all the samples. The band gap decreases with sugarcane leave ash production. FT-IR results showed mainly Si-O-Si bending vibrations and symmetric stretching vibration of Si-O. In addition to this, ~ 494 cm^{-1} and ~ 793 cm^{-1} bands designate to ν_2 symmetric bending of the SO_4^{2-} tetrahedral group and symmetric stretching of Si-O-Si, respectively. Raman spectra showed symmetric stretching of Si-O-Si bond in cristobalite (SiO_2) and O-Si-O bending vibrations. Most importantly, after the addition of sugarcane leave ash, decrease the melting point and increase the tendency to form the glasses. These high optical band gap materials may find some application as resonators and wave guides. Moreover, these waste materials can be used to extract high purity low thermal expansion of coefficient of SiO_2 materials.

Future scope

As the indicated by the results of the present study, the waste material should be utilized as the form of silica in many applications. Additionally, the scanning electron micrographs with energy dispersive spectroscopy will be beneficial to confirm the formation of amorphous /crystalline of the glasses. Moreover, SCLA addition in initial ingredient of glass may lead to form of amorphous nature. However, further study is required to find out the cause of phase separation and its effect on the properties. More importantly, it will be very beneficial for further investigation to know the exact composition and constituents of present samples employing Scanning Electron Microscopy (SEM), Energy Dispersive Spectroscopy (EDS) and Inductive Coupled Plasma (ICP) techniques.

References

[1]. Bronzeoak, *Proc. of international workshop on the utilization of rice husk and rice husk silica, Bangkok* (2003) 1-129.

[2]. S. Asavapisit, N. Ruengrit, *Cem. Conc. Comp*. **27** (2005) 782-787.

[3]. R. Jauberthie, F. Rendell, S. Tamba, I. Cisse, *Constr. build. Mater*. **14** (2000) 419-423.

[4]. C. L Hwang, S. Chandra, *Wast. Mater. Used in Conc. Manufac. USA* **3** (1997) 198-201.

[5]. E. A. Basha, R. Hashim, H. B. Mahmud, A. S. Muntohar, *Constr. Build. Mater.* **19** (2005) 448-453.

[6]. N. Maeda, I. Wada, M. Kawakami, T. Ueda, G. K. D. Pushpalal, *Int. conf. on fly ash, silica fume, slag and natural pozzolans in concrete, Chennai, India* **2** (2001) 835-852.

[7]. H. S. Gheewala, S. Patumsawad, *Eng. Techno.* **3** (2009) 53-56.

[8]. D. G. Cristina, V. Rosa, *Ind. Eng. Chem. Res***. 47** (2008) 4754-4757.

[9]. J. P. Nayak, J. Bera, *National Institute of Technology, Rourkela, Odisha* 769008, *India*.

[10]. K. Seiji, J. Sasaki, *Bio .Techno.* **100** (2009) 3308-3315.

[11]. E. O. Onche, B. I. Ugheoke, S. A. Lawal, U. M. Dickon, *J. Pr. Techno.* **25** (2007) 81-90.

[12]. M. Rozainee, S. P. Ngo, A. Salema, *Bio. Techno.* **99** (2008) 703-713.

[13]. K. G. Mansaray, A. E. Ghaly, *Part A: Recovery, Utilization, and Environmental Effects* **21** (1999) 453-466.

[14]. P. K. Mehta, *Belg. Pat. No*. 802909 (1973).

[15]. J. James, S. M. Rao, *Amer. Ceram. Soc. Bull.* **65** (1986) 1177-80.

[16]. M .A. Hamad, I. A. Khattab, *Thermochim. Act.* **48** (1981) 343-349.

[17]. S. Chandrasekar, K. G. Satyanarayana, P. N. Raghavan, *J. Mater. Sci. Technol.* **38** (2003) 3159-3168.

[18]. S. Sugita, *US Patent No.* **5** (1994). 329867.

[19]. J. Paya, J. Monzo, M. V. Borrachcro, A. Mellado, L. M. Ordoñez, *Cem. Conc. Res.* **31** (2001) 227-231.

[20]. R. F. Pettifer, R. Dupree, I. Farnan, U. Sternberg, *J. Non-Cry. Solids* **106** (1988) 408-412.

[21]. N. Bouzoubaa, B. Fournier, *Materials Technology laboratory, CANMET, Department of Natural resources, Canada* (2001) 1-16.

[22]. M. Nehdi, J. Duguette, A. E. Damatty, *Cem. Concr. Res.* **33** (2003) 1203-1210.

[23]. D. Bui, J. Hu, P. Stroeven, *Cem. Concr. Res*. **27** (2005) 357-366.

[24]. M. H. Zhang, V. M. Malhotra, *Cem. Concr. Res*. **26** (1996) 963-977.

[25]. N. M. Khalaf, A. H. Yousif, *Int. J. cem. Compo. Lig. Weig. Compo.***6** (1984) 241-248.

[26]. K. Ganesan, K. Rajagopal, K. Thangavel, *Constr. Build. Mater.* **22** (2008) 1675-1683.

[27]. A. Boeteng, D. A. Skeete, *Cem. Concr. Res* **20** (1990) 795-802.

[28]. P. Stroeven, D. D. Bui, E. Sabuni, *Fuel* **78** (1999) 153-159.

[29]. K.Y. Foo, B. H. Hameed, *Adv. Collo. Int. Sci* **152** (2009) **39–47**.

[30]. D. M. Ibrahim, M. Helmy, *Thermochim. Act.* **45** (1981) 79-85.

[31]. P. C. Kapur, *Powder Technol.* **44** (1985) 63-67.

[32]. E. Fadaly, *J. Amer. Sci.* (2010).

[33]. S. Chandrasekar, K. G. Satyanarayana P. N. Raghavan, *J. Mater. Sci.* **38** (2003) 3159-3162.

[34]. G. A. Rama Rao, R. K. Sastry, P. K. Rohatgi, *Mater. Sci.* **12** (1989) 469-479.

[35]. P. S. Rakdee, P. Thanmthron, *In Comparison with Other Commercial Fill.* **22** (1998) 154-158.

[36]. Rice hulls could nourish *Silicon Valley Sci. New.* **157** (1994) 194-197.

[37]. G. P. Das, M. M. Rahman, *Int. J. Pest. Man.* **43** (1997) 247-248.

[38]. P. Zhao, X. Guo, C. Zheng *J. Environ. Sci.* **22** (2010) 1629-1636.

[39]. J. P. Nayak, *J. Appl. Sur. Sci.* **257** (2010) 458-462.

[40]. W. H. White, D. M. Burner, B. L. Legendre, *J. Borer: US* 96-1 to US 96-6.

[41]. World paddy production *Food and Agriculture Organization of the United Nations (FAO)* (2012).

[42]. C. A. Browne, R. F. Blouin, *Agric. Exp. Sta. Bull No* **91** (1907).

[43]. A. Pattiya, *Energ. Sour. Part A* **33** (2011) 691-701.

[44]. N. B. Singh, S. Singh, *Int. J. eng. Mater. Sci.* **16** (2009) 415-422.

[45]. J. Moncada, M. M. Ehalwagi, C. A. Química, *C. Manizales, Colombia* **27** (2012) 64-60.

[46]. P. K. Mehta, *U.S. Patent* (1978).

[47]. M. A. Hamad, I. A. Khattab, *Thermochim. Act.* **48** (1981) 343–349.

[48]. S. K. Chopra, S. C. Ahluwalia, S. Laxmi, *Third Workshop on Rice Husk Ash Cements, New Delhi* (1981).

[49]. J. James, M. S. Rao, *Cem. Concr. Res* **16** (1986) 296-302.

[50]. M. S. Surana, S. N. Joshi, *J. Ind. Concr.* **64** (1990) 89-92.

[51]. T. Hiemstra, W. H. V. Riemsdijk, *J. Coll. Interf. Sci.* **136** (1990) 132–150.

[52]. H. P. Wang, K. Lin, Y. J. Huang, *J. Hazard. Mater.* **58** (1998) 147-152.

[53]. Q. J. Yu, K. Sawayama, S. Sugita, M. Shoya, Y. Isojima, *Cem. Concr. Res* **29** (1999) 37-43.

[54]. J. C. Saha, K. Diksit, M. Bandyopadhyay, *International Workshop on technologies for Arsenic Removal from Drinking Water, Bangladesh* (2001).

[55]. S. Huang, S. Jing, J. Wang, Z. Wang, Y. Jin, *Powder Technol* **117** (2001). 232-238.

[56]. S. Asavapisit, N. Ruengrit, *Cem. Concr. Comp.* **3** (2005) 782-787.

[57]. T. I. Watari, A. Nakata, Y. Kiba, T. Torikai, M. Yada, *J. Eur. Ceram. Soc.* **26** (2006) 797-801.

[58]. D. G. Nair, A. Fraaij, A. K. Adri, A. Klaassen, P. M. Kentgens, *Cem. Concr. Res.* **38** (2008) 861-869.

[59]. K. Kordatos, S. Gavela, A. Ntziouni, K. N. Pistiolas, A. Kyritsi, V. K. Rigopoulou, *Microporous Mesoporous Mater.* **115** (2008) 189-196.

[60]. J. P. Nayak, J. Bera, *J. Met. Mater. Miner.* **19** (2009) 15-19.

[61]. C. Bhavornthanayod, P. Rungrojchaipon, *J. Met. Mater. Miner.* **19** (2009) 79-83.

[62]. S. Rukzon, P. Chindaprasirt, R. Mahachai, *Int. J. Min. Metall. Mater.* **16** (2009) 242-245.

[63]. R. U. Lakshmi, V. C. Srivastava, I. D. Mall, D. H. Lataye, *J. Environ. Man.* **90** (2009) 710-720.

[64]. S. Jennifer, L. Blond, J. C. Horwell, B. J. Williamso, C. Oppenheimer, *J. Environ. Mon.* **12** (2010) 1459-1470.

[65]. F. Adam, J. N. Appaturi, R. Thankappan, M. Asri, M. Nawi, *Appl. Surf. Sci.* **257** (2010) 811-816.

[66]. M. M. Haslinawati, K. A. Matori, Z. A. Wahab, H. A. A. Sidek, A. T. Zainal, *Int. J. Bas. Appl. Sci.* **9** (2010) 245-248.

[67]. F. W. Bondioli, L. Barbieri, A. M. Ferrari, T. M. Fredini, *J. Am. Ceram. Soc.*, **93** (2010) 121-126.

[68]. Y. Ruangtaweep, J. Kaewkhao, C. Kedkaewand P. Limsuwan, *Pro. Eng.* **8** (2011) 58-61.

[69]. A. Dongmin, Y. Guo, B. Zou, Y. Zhu, Z. Wang, *Biomass Bioenergy* **35** (2011) 1227-1234.

[70]. T. Liou, C. Yang, *Mater. Sci. Eng.* **176** (2011) 521-529.

[71]. R. P. Singh, H. Singh, *Int. J. Eng. Sci. Techno.* **3** (2011) 10-13.

[72]. O. O. Amu, S. A. Ogunniyi, O. Oladeji, *J. Sci. Ind. Res***. 2** (2011) 323-331.

[73]. T. Wasanapiarnponz, B. Vorajesdarom, E. Rujirakamort, S. Nilpairach, C. Mongkolkachit *Mater. Sci. Eng.* **18** (2011) 222028.

[74]. R. Zerbino, G. Giaccio, O. R. Batic, G. C. Isaia, *Constr. Build. Mater.* **36** (2012) 796-806.

[75]. W. Y. Tommy, S. Ali, *Constr. Build. Mater.* **29** (2012) 541–547.

[76]. F. Andreola, M. I. Martın, A. M. Ferrari, I. Lancellotti, F. Bondioli, M. Rincon, M. Romero, L. Barbieri, *J. Cera. Int.* **7** (2008) 230-234.

[77]. S. Tuscharoen, J. Kaewkhao, P. Limsuwan, W. Chewpraditkul, *Proc. Eng.* **32** (2012) 734-739.

[78]. E. P. Ayswarya, K. F. Vidya Francis, V. S. Renju, E. T. Thachi, *Mater. Des.* **41** (2012) 1-7.

[79]. L. Behak, W. P. Nunez, *Mater. Pav. Des*. **6** (2013) 3251-3255.

[80]. R. M. Mohamed, I. A. Mkhalid, M. A. Barakat, *Arab. J. Chem.* (2013) 252-256.

[81]. K. Xu, Q. Sun, Y. Guo, S. Dong, *Appl. Surf. Sci.* **276** (2013) 796-801.

[82]. O. Olawale, A. Akinmoladun, I. Oyawale, A. A. Rejoice, *Int. J. Sci. Eng. Res.* **4** (2013) 564-571.

[83]. D. A. Skooget, *Principles of instrumental analysis*, fifth edition, Harcourt Publishers, (2000).

[84]. P. Misra, M. Dubinskii, *Ultraviolet Spectroscopy and UV Lasers*, Editors, Marcel Dekker, New York (2002).

[85]. H. Lehmann, R. Gatzke, *Dilatometrie and differential thermal analysis for the evaluation of processes* (1956).

[86]. D. M. Hatch, S. Ghose, *Phys. Chem. Minerals* **17** (1991) 554-562.

[87]. W. A. Deer, R. A. Howie, W. S. Wise, *Geol. Soc.* 22 (2004).

[88]. I. Weber, U. Bottger, E. K. Jessberger, H. W. Hubers, S. G. Pavlov, S. Schroder, N. Tarcea, T. Dorfer, *43rd Lunar and Planetary Science Conference* (2012).

[89]. F. Ahangaran, A. Hassanzadeh, S. Nouri, *Int. Nan. Let*. (2013).

[90]. S. H. Javed, F. H. Shah, M. Mansa, J. fac. Eng. Techno. **18** (2011) 39-46.

[91]. I. P. Swainson, M. T. Dove, D. C. Palmer, *Phys. Chem. Miner*. **30** (2003) 353-356.

[92]. S. C. Cherukuri, L. D. Pye, I. N. Chakraborty, R. A. Condrate, J. R. Ferraro, B. C. Cornilsen, K. Martin *Spectra. Let.* **18** (1985) 123-13.